

MINERAL EXPLORATION POTENTIAL OF ERTS-1 DATA

W. A. Brewer, M. C. Erskine, Jr., W. T. Haenggi, R. O. Prindle
Earth Satellite Corporation
2150 Shattuck Avenue
Berkeley, California 94704

June 4, 1974
Type III Final Report

Prepared for
GODDARD SPACE FLIGHT CENTER
Greenbelt, Maryland 20771

Reproduced by
**NATIONAL TECHNICAL
INFORMATION SERVICE**
US Department of Commerce
Springfield, VA. 22151

(E74-10608) MINERAL EXPLORATION POTENTIAL
OF ERTS-1 DATA Final Report (Earth
Satellite Corp., Berkeley, Calif.)
CSCL 086

63/13

Unclas
00608

N74-28841

1. Report No. 2	2. Government Accession No.	3. Recipient's Catalog No.
4. Title and Subtitle Mineral Exploration Potential of ERTS-1 Data		5. Report Date June 4, 1974
		6. Performing Organization Code
7. Author(s) <u>W.A. Brewer, M.C. Erskine, Jr.,</u> <u>R.O. Prindle, W.T. Haenggi</u>		8. Performing Organization Report No. 2
9. Performing Organization Name and Address Earth Satellite Corporation 2150 Shattuck Avenue Berkeley, California 94704		10. Work Unit No.
		11. Contract or Grant No. NAS5-21745
12. Sponsoring Agency Name and Address Goddard Space Flight Center Greenbelt, Maryland 20771		13. Type of Report and Period Covered Type III Final Report
		14. Sponsoring Agency Code
15. Supplementary Notes		
16. Abstract ERTS imagery of an area approximately 15,000 square miles in Arizona was interpreted for regional structure and tectonic units. Eight fault systems were identified by trend, of which two, Northeast and Northwest, are considered to be related to porphyry copper mineralization. Nine tectonic units can be identified on the imagery as distinct geological identities. The boundaries between these units can be correlated with theoretical shear directions related to the San Andreas stress system. Fourier analysis of the N50°W fault trend indicates a fundamental spacing between Fourier energy maxima that can be related to distances between copper deposits.		
17. Key Words (Selected by Author(s)) Arizona; porphyry copper deposits; tectonics; Fourier analysis of faulting		18. Distribution Statement
19. Security Classif. (of this report) Unclassified	20. Security Classif. (of this page) Unclassified	

*For sale by the Clearinghouse for Federal Scientific and Technical Information, Springfield, Virginia 22151.

PREFACE

- (a) Objective: The objective of the project is to determine if ERTS imagery can be used for mapping regional tectonic structures that previously were not known or mapped, that in turn can be used to locate porphyry copper mineralization.
- (b) Scope of Work: ERTS imagery was analyzed for lineations and regional tectonic features. Interpretations were then analyzed in terms of their relationships to published geological, tectonic and geophysical maps and porphyry copper locations. In areas of known hydrothermal alteration, comparisons between natural color and color infrared underflight photography and ERTS color composites were undertaken.
- (c) Conclusions: The Arizona ERTS imagery is very advantageous in interpreting and mapping regional structure trends and tectonic units that are not readily mapped by other techniques. Interpretations of hydrothermal alteration are much more difficult than structural mapping.
- (d) Summary of Recommendations: It is recommended that the published tectonic maps be updated by incorporating interpretations performed on ERTS imagery.

Preceding page blank

CONTENTS

Text

INTRODUCTION	1
ERTS IMAGERY	3
ERTS LINEATION STUDY	7
Optical Measurements of Fault Frequency	9
TECTONICS	12
COMPARISON OF ERTS IMAGERY WITH THAT BY OTHER REMOTE SENSORS	28
Side-Looking Airborne Radar (SLAR)	28
Apollo Photography	31
Colored Aerial Photography	34
Aeromagnetics	37
FIELD CHECK	39
SUMMARY AND CONCLUSIONS	41
REFERENCES CITED	45

TABLES

Table 1	Comparison Between Theoretical and Actual Shear Directions . . .	18
Table 2	Spacing Between Selected Porphyry Copper Deposits	22

ILLUSTRATIONS

Fig. 1	Location of ERTS Frames Used in Mosaic	2
Fig. 2	Regional Structural Analysis	16
Fig. 3	Fourier Energy Spectrum (N50°W Lineations) Latitude Data	24
Fig. 4	Fourier Energy Spectrum (N50°W Lineations) Longitude Data. . . .	25
Fig. 5	Histogram Showing the Number of Times a Maxima Occurs on the Fourier Transforms of Photolinear Data Versus the Harmonic Spacing of Those Photolinears	26
Fig. 6	Side-Looking Radar Coverage	29
Fig. 7	Apollo Photo Coverage	32
Fig. 8	Apollo Photo Structural Raw Data	33
Fig. 9	Apollo Photo Emphasizing EW Structures	35

LIST OF PLATES *

- Plate 1 Outcrop Map as Seen on ERTS-MSS Mosaic
- Plate 2 Structure Map (Compiled Data)
- Plate 3 Known Porphyry Copper Deposits, Mineral Occurrences, Laramide Intrusions, Tectonic Units and Regional Lineations
- Plate 4 Combined and Simplified Interpretation of ERTS-MSS Mosaic for Geologic Structure
- Plate 5 Relative Intensity of N45°E Lineations Determined by Photocell Survey of ERTS Interpretation of NW and NE Structures
- Plate 6 Relative Intensity of N50°W Lineations Determined by Photocell Survey of ERTS Interpretation of NW and NE Structures
- Plate 7 Relative Intensity of N70°E Lineations Determined by Photocell Survey of ERTS Interpretation of NS and EW Structures
- Plate 8 Relative Intensity of N-S Lineations Determined by Photocell Survey of ERTS Interpretation of NS and EW Structures
- Plate 9 Relative Intensity of N25°W Lineations Determined by Photocell Survey of ERTS Interpretation of NW and NE Structures
- Plate 10 Relative Intensity of N75°W Lineations Determined by Photocell Survey of ERTS Interpretation of NS and EW Structures
- Plate 11 Relative Intensity of E-W Lineations Determined by Photocell Survey of ERTS Interpretation of NS and EW Structures
- Plate 12 Bouger Gravity and Configuration M-Discontinuity
- Plate 13 Alteration Study
- Plate 14 Structural Interpretation from Aeromagnetic Data

* Plates are attached at end of report.

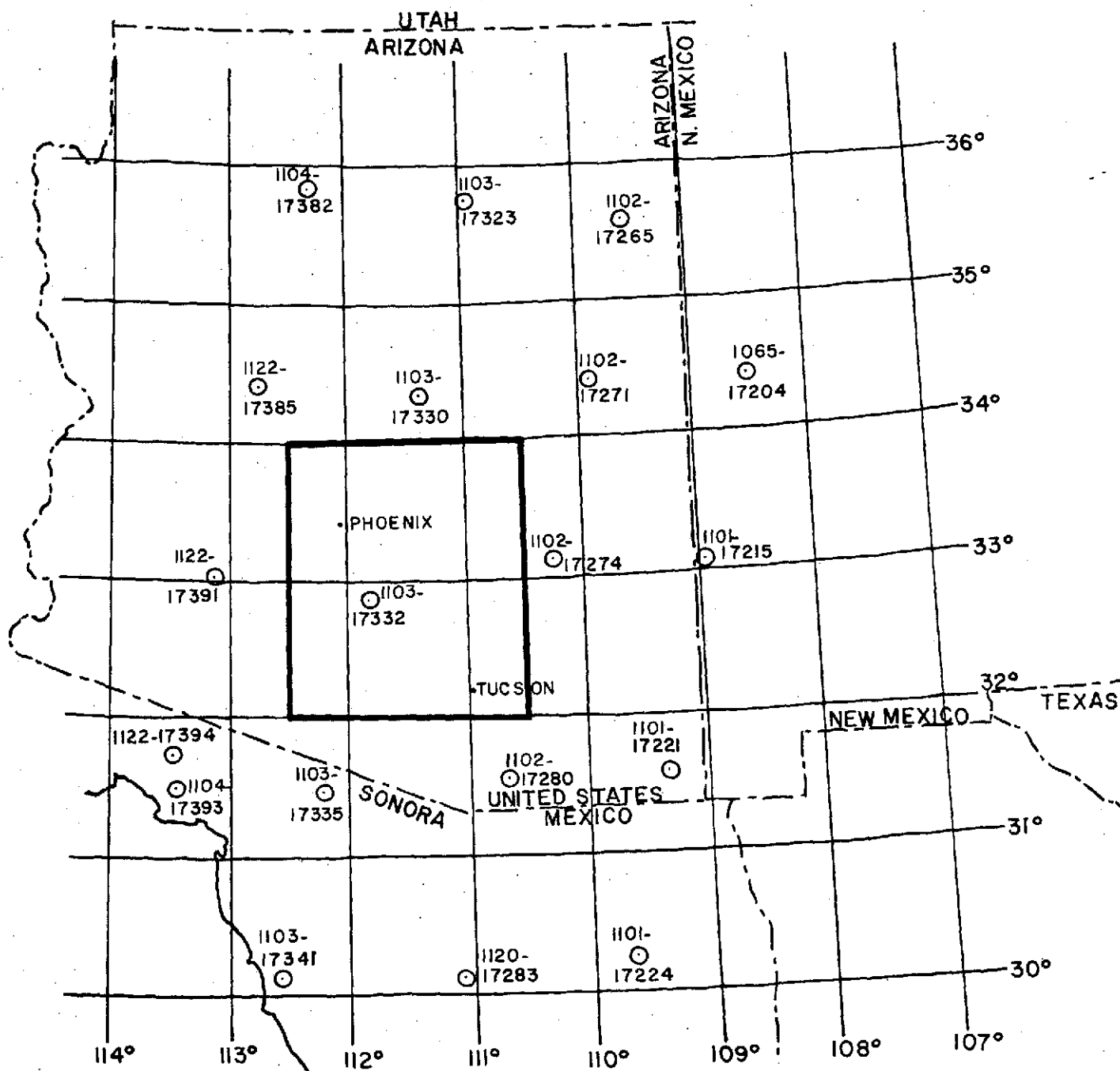
INTRODUCTION

The purpose of this investigation is twofold:

1. Evaluation of the use of ERTS imagery as an aid to or replacement of other higher resolution data sources used in mineral exploration.
2. Evaluation of the synoptic character of ERTS imagery as applied to mineral exploration.

We found that ERTS imagery yields data which can be used to rapidly compile small-scale geologic and tectonic maps for regional evaluation to select exploration areas but may have only limited use for locating and defining specific target areas. Nevertheless, mathematical analysis of lineation data, which can be gathered rapidly from ERTS imagery, shows promise for development of parameters for defining specific targets.

The test site for this study is located in central Arizona and comprises approximately 15,000 square miles (Figure 1).



EXPLANATION

SCALE 1:5,000,000

1104-
○ CENTER OF ERTS FRAME & PHOTO
17382 IDENTIFICATION NUMBER

— TEST AREA

Figure 1 LOCATION OF ERTS FRAMES
USED IN MOSAIC

ERTS IMAGERY

With the advent of ERTS it has become possible to achieve an overview of a tectonic province never before available to the exploration geologist and areas of 180 x 180km at a useful scale of 1:1,000,000 are readily available for analysis. In addition four filtered bands may be studied and the spectral contrasts of vegetation utilized (as in MSS bands 4 and 5) or diminished (as in MSS bands 6 and 7), to enhance the geological textures of the terrain. Finally, with aspects not yet even fully appreciated by geologists, ERTS supplies a seasonal view, a view with varying solar illumination angles to enhance topography, and last, but not least, quantifiable imagery taken with the same sensor system everywhere in the world.

Within the study area, the only exposed rock units that can be reliably identified and mapped on the imagery are dark-colored, sparsely-vegetated, Tertiary and Quaternary basaltic volcanic series.

Careful and objective photogeologic methods applied to ERTS imagery for determination of faults and outcrops and subsequent comparison of ERTS data with existing geological, tectonic and structural maps presented by the U.S. Geological Survey and Arizona Bureau of Mines shows that ERTS imagery allows markedly advantageous interpretations with regard to: (1) regional structure (essentially the pattern of faults), (2) "bedrock" outcrop delineation from alluvial cover and recognition of shallow alluvial cover, and (3) correlation of exposed and unexposed regional features over relatively great distances. Plate 1 compares ERTS-mapped outcrop patterns with those of published data.

Subsidiary and residual geologic advantages obtained by using ERTS data are: (1) geographic accuracy, and (2) determination of general regional geologic framework in areas where no other data exist. The greatest overall usefulness of ERTS imagery centers on its usefulness in tying together existing fragmentary data from various sources into a coherent regional interpretation.

Considerable trouble in accurate determination of the specific position of geological features noted on ERTS imagery with respect to published maps was encountered during the project. Part of the difficulty is because ERTS imagery is presented as a Universal Transverse Mercator (UTM) projection and most published maps are on other projections. Problems inherent in comparing data depicted on various projections were underestimated during early stages of the project and the result is that our overlays did not align perfectly.

The location problems discussed above are relatively insignificant for regional geological studies but become critical when ERTS imagery interpretation is applied to mineral exploration. The resolution capacity of ERTS imagery for linear geological features (bedding, faults, fractures, foliation trends, sills and dikes), which are often associated with mineral occurrences, is great enough to justify the effort to accurately locate the features on existing maps.

Furthermore, mineral exploration targets (prospects, small mines, etc.) frequently occur within limited areas (less than 10 square miles) and errors in location due to uncontrolled transfer of data from ERTS imagery to existing maps can cause serious problems to an exploration program.

Accurate locations are especially necessary when geophysical surveys are designed. In such surveys it is desirable for cost reasons to minimize the area to be investigated but essential to survey all of the prospective area.

A solution to the location problem is to use scales larger than 1:1,000,000 for ERTS imagery interpretations. The resolution capacity of the imagery is sufficient to justify work designed for mineral exploration at scales of 1:500,000 or 1:250,000. Known geographic features are recognized more readily on the larger scale imagery than the 1:1,000,000 scale which permits more accurate transfer of location data from existing maps to ERTS.

Fault data derived from ERTS imagery are in good agreement with structures shown on existing geologic maps and with the results of other structural studies made from airborne and space remote sensing data. Plate 2 shows faults indicated on the Tectonic Map of the United States (1962) and the Geologic Map of Arizona (1969) for comparison with ERTS-derived data. When Plate 4 is overlayed on this map, it is obvious that more faults are shown by the ERTS studies at 1:1,000,000 scale than is feasible to show on conventional maps at the same scale. This difference reflects the synoptic view of ERTS imagery in a spectacular manner. The difference is largely due to limited sample areas in previous studies, and inability of conventional field and photogeological methods to integrate data over large areas and to distinguish through-going faults in covered areas.

Almost all faults shown on the existing tectonic maps were identified on the ERTS imagery. Variations in location of faults are attributed to differences in projections between ERTS imagery and published maps. Published maps used in our studies are: (1) Tectonic Map of the United States (1962), conic projection, enlarged from 1:2,500,000 to 1:1,000,000, and (2) Geologic Map of Arizona (1969), Lambert conformal conic projection, reduced from 1:500,000 to 1:1,000,000. Low-angle faults of the test area are difficult to recognize on ERTS imagery although segments of thrust faults are recognized.

A combination of ERTS fault and outcrop interpretations with published data will result in a more detailed and accurate tectonic map at a scale of 1:1,000,000 for the study area.

We recommend that existing tectonic maps of the area be reviewed and revised to reflect data available from ERTS imagery.

ERTS LINEATION STUDY

Numerous authors have postulated a relationship between locations of ore deposits in the western United States and intersections of fault zones, orogens (linear, deformed regions) and tectogenes (long, narrow down warps). In southeastern Arizona, Billingsley and Locke (1949), Mayo (1958), Schmitt (1966), and Wertz (1970) have published data attempting to show relationships between porphyry copper deposits and structural intersections.

We have analyzed fault data derived from studies of ERTS imagery, utilizing both qualitative and quantitative approaches, in an attempt to demonstrate relationships between spacing, trend and intersections of lineations to porphyry copper locations and crustal thickness.

For this study linear features observed on ERTS imagery were interpreted, without reference to published data, as fault traces. Imagery from MSS bands 6 and 7 was joined into a mosaic and the interpretation recorded on transparent overlays. All work with ERTS data was done on a scale of 1:1,000,000.

To minimize bias, imagery was interpreted for each significant fault system direction individually. In the interpretation process, work was done over relatively small areas and coverage of the mosaic was by quadrants and sectors with frequent rotation of the mosaic. A further means of reducing bias in interpretation of the data was a deliberate effort to avoid noting large through-going features initially. These features tend to become "real" to the interpreter and also tend to preclude observation of actual, but poorly-defined lineations which cross, contradict or obviate them.

The relatively low MSS resolution makes distinction between fault related lineations and those caused by bedding and foliation difficult. As a result, the final interpretation may incorporate a considerable number of lineations due to bedding and foliation.

Two mosaics of imagery in bands 6 and 7 were interpreted for fault structure. Two composite overlays were compiled showing: (1) North-South and East-West lineations, and (2) Northwest-Southeast and Northeast-Southwest lineations. From these composites an interpretation was compiled by deleting insignificant lineations, intensifying major lineations and adding faults mapped on the ground at porphyry copper locations (Plate 4).

It was apparent at the outset that repetitions of strike directions on isolated fault segments indicate that regional systems are operative in the area. Eight systems were recognized:

1. System "A" N40°E to N50°E. Remarkably straight and persistent quite continuous (but made up of very short segments), at least as visible to the interpreter in MSS imagery. Schmitt (1966) correlates this direction with older Precambrian-through-Cretaceous activity. It appears to be considerably offset by other systems of East-West and Northwest trends.
2. System "B" N50°W. Similar overall to system "A."
3. System "C" N35°W. Curves into and out of system "B" faults and fractures. Includes much (young) Basin-and-Range high-angle faulting and at the same time it projects roughly toward the Las Vegas-Walker Lane systems to the Northwest.
4. System "D" N65°E to N75°E. Very short individual segments, yet remarkably persistent across the study area and spaced about 20 miles apart.
5. System "E" N-S \pm 10°. Rather sinuous and complex. In some areas dominant, and in others nearly obliterated. Appears to include many elements of both the Wasatch-Jerome and Front Range Orogens as described by Schmitt (1966), but there is the strong suggestion also that another (older?) subparallel North-South "system" has been somehow incorporated.

6. System "F" N25°W (average). Curves toward the south. This trend plots very closely on or parallel with Schmitt's Wasatch-Jerome axis, and has previously been used to "explain" Miami-Inspiration, Ray, San Manuel and other porphyries.
7. System "G" N75°W (average). Curves toward the south. This is the Texas zone (or Texas Orogen) described by Schmitt and others, and plots very closely to the trend shown on Schmitt's maps. However, it is apparent that there are (older?) associated subparallel trends (system "H") which it has "utilized."
8. System "H" close to E-W. This system has strikes averaging within a few degrees of East, but its segments are both highly offset by other systems and markedly curved at their ends, the radii of curvature being on the order of 100 miles.

In addition to the eight identifiable fault systems, other local or anomalous structural trends (correlatable with Basin-and-Range topography) are present in the study area.

Optical Measurement of Fault Frequency

To determine relative intensity of lineations for the fault systems noted on ERTS imagery, a photocell measuring system was devised. Intensity measurements were taken at points on a grid system covering the test area for systems "A," "B," "D," "E," "F," "G," and "H" of the ERTS lineation survey at a scale of 1:1,000,000. Data were not gathered for system "C" because the photocell could not distinguish or obtain accurate resolution of this trend. The data resulting from this measuring approach were plotted (at the same scale) as contoured values of light intensity (Plates 5, 6, 7, 8, 9, 10 and 11).

Photographic negatives of two ERTS overlays showing North-South and East-West lineations and showing Northwest-Southeast and Northeast-Southwest lineations were prepared at scales of 1:1,000,000. Two identical negatives for each separate overlay were prepared and

superimposed. One negative of the "sandwich," thus formed, was offset slightly (1.3mm) along the direction to be studied. This, in effect, is a directional filter (Blanchet, 1967); linears parallel to the direction of offset will transmit light with undiminished efficiency but linears in other directions will be blocked out by such a movement and transmittance will in effect be zero. The negatives were then placed over a uniform light source (Richards MIM-335100 Light Table). The result is that light passes through the "sandwiched" negatives only along lines depicting the direction being studied.

A Gossen Luna-Pro light meter was used as the sensor and was affixed to a movable bridge over the light table at a constant distance from it. A coordinate system for determination of geographic location on the negatives was overlaid on the negatives and removed prior to taking each reading. On the 1:1,000,000 scale used, the smallest area sampled by this system was an 8-mile (12.87km) square. Accordingly, a mask was prepared from opaque paper which permitted only light from such an area to pass from source to sensor. Readings were taken in a darkroom and exposure time was 10 seconds for each grid point located at the center of the square filter. Scale readings ranged between 0 and 9, which is equivalent to 0-to-4 foot candles.

The data resulting from this mechanical procedure is essentially a digitized grid with an 8-mile unit period representing the intensity of fracturing in a particular strike direction. This data may then be transformed by the Fourier Transform pair (Stratton, 1941):

$$F(f) = \frac{1}{\sqrt{2\pi}} \int_{x_1}^{x_2} I(x) e^{-ixf} dx \quad (\text{Eq. 1})$$

$$I(x) = \frac{1}{\sqrt{2\pi}} \int_{f_1}^{f_2} F(f) e^{-ixf} df \quad (\text{Eq. 2})$$

where:

$I(x)$ = the transmittance of a point x along a given data line (the intensity of fracturing), and

$F(f)$ = the intensity of faulting at a fault spacing of f along the same line of data.

The Fourier analysis then is a means of relating fault intensity to fault spacing. For example, if in a given area the intensity of the major faults is related to crustal thickness, then we should see a systematic change in the locations of the maxima of the $F(f)$ curve with crustal thickness over the data block. A second possibility is that in a given region, fault zones that penetrate the crust and thus define crustal blocks would occur with one spacing and those of lesser extent within the crustal blocks would occur with another spacing; thus, perhaps the method can help us define the crustal blocks and their boundaries. It seems probable that mantle-derived material would reach the surface along the boundaries of these crustal blocks.

TECTONICS

Using ERTS imagery mosaics at a scale of 1:1,000,000, we divided most of Arizona and adjacent parts of the states of Nevada, California, New Mexico, Utah, and Sonora (Mexico) into tectonic units. Within and adjacent to the test area, nine such units were recognized (Plate 3).

Our basis for differentiation of tectonic units is based on "tectonic style" which can be related to the total character of a group of related mesoscopic (as observed on ERTS imagery) features. Principal criteria used in defining the tectonic units are as follows:

1. Orientation of linear parallel and subparallel features
2. Density of structural, stratigraphic and geomorphic features
3. Relief
4. Relative abundance of rock types
5. Mode of deformation
6. Recognizable features which cannot be precisely defined in geometric terms.

Characteristics of the nine tectonic units shown on Plate 3 taken from the ERTS mosaic are:

Unit I--High ratio of mountainous area to valley area (about 5:1); sharp, well-developed relief; ranges and valleys trend north; spacing between valley areas averages 45km, except in extreme north where spacing is 15 to 20km; numerous major lineations crossing topographic trends at N50°W to N70°W and N40°E to N50°E; well-developed dendritic to rectilinear drainage; common evidence of volcanism (cones, basalt flows); numerous intrusions.

Unit II--Low ratio of range area to fill area (1:3); distance between valley axes about 38km; extensive pediment development; relatively low relief; north trending ranges and valleys; regional lineations trending N65°E to N70°E across structures within the unit; numerous intrusions.

Unit III--Elongated ranges and valleys trending N35°W to N40°W; low ratio of narrow range area to broad valley area (approximately 1:2.5); spacing between valley axes 15 to 20km; very few structures across range trends; local centers of recent volcanic activity (basalt flows); many ranges with foliation and/or fault/fractures trending N50°E to N60°E (confined to ranges); bounded on west by San Andreas Fault zone and Gulf of California; northern boundary is Gila-Salt River Lineament trending N67°E.

Unit IV--Similar to Unit III except some ranges and valleys oriented N55°W to N60°W and less persistent orientation and spacing of ranges, foliations, and faults, with northern boundary being Gila-Salt River Lineament.

Unit V--Very low ratio of range area to valley area (< 1:10); numerous N65°E to N70°E lineations entering area from units II and VI.

Unit VI--Relatively few ranges and valleys with 1:1 ratio between range and valley areas; sharp, rugged relief in mountains; ranges and valleys trend N45°W, en-echelon arrangement of ranges; 38km average distance between major valley axes; relatively few through-going lineations, but numerous lineations trending N65°E to N70°E in western half of unit; numerous intrusions.

Unit VII--High ratio of range areas to valley areas (5:1); crude alignment of valleys and range crests of N30°W; 38km spacing between major valley axes; rugged, sharp relief; ill-defined northern boundary; southern boundary strongly controlled by Gila-Salt River Lineament; rectilinear drainage pattern grading to dendritic; few through-going lineations and those present trend N30°W.

Unit VIII--Elongated ranges trending N55°E to N60°E; range to valley area ratio of 1:2; valley axes spaced at 19km intervals; very well-defined northeast and southwest boundaries trending N35°W to N40°W; irregular southern boundary controlled by Gila-Salt River Lineament.

Unit IX--Poorly-defined elongated ranges and valleys with range valley area ratio 1:3; major valley axes about 50km apart; extensive pediments; strong structural grain N55°W; well-defined boundary with unit VIII at N35°-N40°W and with units III and IV along Gila-Salt River Lineament at N67°E.

We have demonstrated that tectonic units can be readily delineated by the use of ERTS imagery where parameters that otherwise cannot be viewed in their entirety are mesoscopic. The units described have properties similar to Polygonal Crustal Blocks described by Cloos (1939).

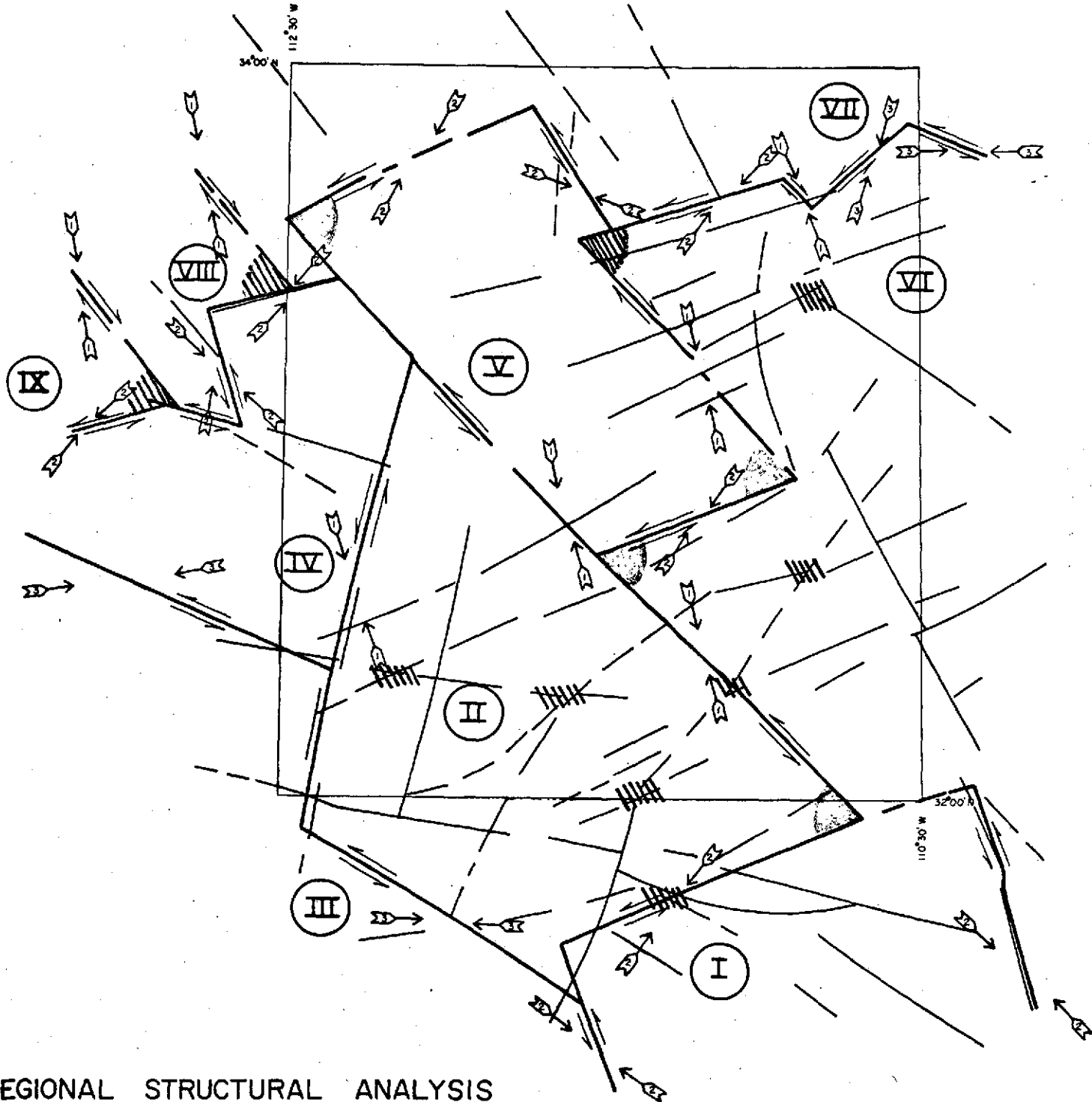
Light-intensity maps of lineation systems (Plates 5-11) have been compared to known porphyry copper localities in an effort to demonstrate a relationship between mineralization and tectonics as interpreted from various properties of the linear elements. We tried numerous methods of analysis of the data but were unable to demonstrate a significant correlation between lineation intensity, fault alignment or structural intersections to porphyry copper localities.

Some methods used were:

1. Overlay of lineation intensity maps to evaluate trends, intensity values, and intersection of trends with known porphyry copper deposits (using individual intensity maps and combinations of them).
2. Overlay of lineation intensity maps and residual magnetic map to edit data gathered by intensity overlay.
3. Overlay of lineation intensity and magnetic maps with maps showing Laramide rocks (especially intrusive igneous rocks).
4. Overlay of all maps on metallogenic maps.
5. Fourier analysis of optically-derived fault intensity data (photo linear).

These exercises did not yield definite conclusions, but there is a fair spatial correlation between the high intensity contours (6 and 7) on the N70°E and N-S intensity maps (Plate 7 and 8), porphyry locations, Laramide intrusions (Plate 3), and anomalies on the Residual Aeromagnetic Map of Arizona by Sauck and Sumner (1972). These locations of correlation are shown as prospective areas on Plate 3. Unfortunately these areas do not direct exploration to all of the known deposits, and the "prospective" areas are quite large. Above all, the "prospective" areas can also be defined using regional magnetic surveys and available geologic maps. In other words, ERTS imagery studies are of secondary use in this sense for studies in Arizona. However, in less-known parts of the world ERTS imagery can supply data on regional geology to assist in defining "prospective" areas.

Analysis of the tectonic units recognized in the test area seems promising for development of a coherent regional model which, in turn, can be used as a guide for location of porphyry copper deposits. Figure 2 shows a model derived from a theory of strike/slip faulting described by Moody and Hill (1956). A model based on theories of the "New Global Tectonics" was also considered. Seafloor spreading theories account for the San Andreas Fault as a transform, but our extension of the plate tectonics model to the test area did not adequately explain the interpreted tectonic data.



REGIONAL STRUCTURAL ANALYSIS

EXPLANATION

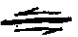

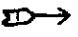
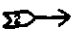
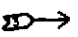


-  Tectonic Unit Boundary, showing sense of motion along decouple.
-  Regional Lineament
-  Primary Stress Direction
-  Secondary Stress Direction
-  Tertiary Stress Direction
-  Key Angle
-  Prospective Areas for Mineralization

Figure 2

16

In our model we assume that:

1. The San Andreas Fault is a primary right-lateral strike/slip fault caused by regional compressive forces with the principal stress horizontal and aligned N10°W.
2. The area shown on Figure 2 is tectonically related to the San Andreas Fault and has been since the inception of the fault, thus, it is subjected to regional compression with the principal stress aligned N10°W.
3. The stress system now operative has been in existence since inception of the San Andreas Fault which was probably during the Cretaceous Period.
4. The dihedral angle of shear for rocks in the area averages 60°.
5. Second, third, fourth and lower order stress systems have developed which cause strike/slip faults or linear features aligned along the theoretical directions of shearing to develop. The acute bisectrix of secondary and lower order shear zones with their parental zones is $90^\circ - \gamma$ where γ ranges between 0° and 30° and averages 15°.
6. Boundaries of tectonic units are decoupled zones aligned along theoretical shear directions.

Figure 2 shows first, second, and third order stress directions derived from the assigned tectonic unit boundaries and relative motions along boundaries. Table 1 shows a comparison between directions derived from Figure 2 and theoretical directions derived from using the San Andreas direction as a primary right-lateral shear.

Table 1

COMPARISON BETWEEN THEORETICAL AND
ACTUAL SHEAR DIRECTIONS

San Andreas (Assumes N40°W trend for San Andreas Fault)	Tectonic Unit Boundaries Arizona Model
<u>First-Order Directions:</u>	
Right lateral N40°W	N38°W to N45°W
Left lateral N20°E	N14°E
<u>Second-Order Directions:</u>	
Right lateral N5°E	Absent
Right lateral N85°W	Absent
Left lateral N25°W	N17°W
Left lateral N65°E	N65°E to N75°E
<u>Third-Order Directions: *</u>	
Right lateral N50°E	N45°E
Left lateral N70°W	N57°W to N70°W

* First-order features are repeated in third order and all orders lower are composed of repeats of directions in 1st, 2nd, and 3rd orders

The model is generalized and no attempt is made here to resolve discrepancies between the theoretical directions (San Andreas) and those observed. Factors that should be evaluated in a critical test of the model are:

1. Effect of anisotropy in the stressed plate on shear directions (the theory assumes homogeneity of the plate).
2. Effects of structural elements created during stress regimes existing prior to the "San Andreas" system on trend of shear directions.
3. Possibility of changes of orientation of principal regional stress during the history of the system.
4. Compatibility of our interpretation of the San Andreas Fault as a strike/slip fault and theories of the "New Global Tectonics" which regard it as a transform fault.

The model is presented as an example of the type of tectonic analysis that can be performed with the aid of ERTS imagery using the concept of tectonic style. It differs from most previous models in that primary activities of such famous "continental" features as the Texas Lineament, Wasatch-Jerome Axis, Walker-Lane, etc. are not necessary to explain observed features, and in its emphasis of the San Andreas system. This does not mean that we negate the importance of these features (Tectonic Unit VIII is the Walker-Lane), but that we feel the model can be used to explain regional structure and history of mineralization and appears to permit us to predict structural relationships without using features other than the San Andreas Fault as controlling factors. A prime objective of our study is to show how ERTS imagery can be utilized in mineral exploration; hence, comparison of our model and porphyry copper localities shows that clusters of porphyries at Globe-Miami and around the Sierrita Mountains occur within acute angles formed by intersections of tectonic unit boundaries. In our model these angles are formed where

right-lateral and left-lateral "shears" intersect with relative motion directions away from the junction, along the intersecting boundaries. The resultant system sets up an area of low intensity within the regional stress field which results in relative extension. The extension zones act as foci for intrusive igneous activity and subsequent or contemporaneous mineralization. In effect, it is postulated that the crust is "stretched" and highly susceptible to rupture in these areas.

In addition to the Globe-Miami and Sierrita Mountains areas, porphyry copper deposits at San Manuel and Posten Butte occur within reasonable distances of similar tectonic-unit junctions. Other prospective areas, with no known porphyries, are near the Key Angle intersections (Figure 2) of units V and VI, IV and VIII, and IV and IX, north and west of Phoenix.

If the model is used as an exploration guide, all areas within acute angles formed by lineations (faults) trending NW and N65°E to N75°E are prospective for porphyry copper deposits. The prospective intersections do not have to be features bounding the tectonic units but can occur anywhere in the areas as shown in Figure 2.

Our model is not a complete guide to the explorationist and the discussions on why porphyry copper deposits occur within the regional framework are subject to much debate. ERTS imagery studies are unlikely to result in answers to questions on why one Laramide intrusion is mineralized and another is not, but can--because of the synoptic nature of ERTS data--assist the explorer in putting together regional concepts to guide his search.

Porphyry copper tectonic maps can be constructed and ERTS imagery studies can provide much of the data for their preparation. A map of this type should show interrelationships between all features of an area that are known to exert control on mineralization. Essential components are:

1. Structural data--tectonic units, faults, folds with emphasis on directions, types of faults, and relationships known to control mineralization.
2. Intrusions--ages, rock types, sizes, shapes, relationships to mineralization where known, relationships to contemporaneous extrusive rocks.
3. Metal occurrences--known deposit locations, types of deposits, alterations, emphasis on copper, lead, zinc, silver, gold, molybdenum.
4. Regional magnetics, crustal data (gravity and seismic).

Of these basic components to porphyry copper tectonic maps, ERTS imagery can contribute an accurate base; 80 to 90 percent of the useful structural data and a relatively small amount of data on intrusions and extrusions (verification of shape, location and size). We feel the tectonic map concept is an effective exploration tool and have demonstrated here how data derived from ERTS imagery can and cannot be used in compilation of the map.

At the outset of our investigation a seeming regularity of distances, along azimuths, between some porphyry copper deposits was observed (Table 2). Our studies of ERTS imagery show some systematic spacings of fault zones, especially in systems "A" (N40°E to N50°E) and "B" (N50°W). These observations suggest a relationship between loci of porphyry copper deposits and fundamental spacings of fault zones.

An experiment utilizing Fourier analysis was designed to quantify relationships between lineation spacings and to determine effects of

Table 2

SPACING BETWEEN SELECTED PORPHYRY COPPER DEPOSITS

Deposits	Bearing	Spacing (Miles)		
		n	2n	m
Ajo - Vekol	N71°E		50.2	
Sacaton - Posten Butte	N76°E	24.2		
Posten Butte - Ray	N70°E	26.4		
Silver Bell - San Manuel	N68°E		52.9	
Copper Creek - Safford	N76°E		51.7	
Sacaton - Silver Bell	N25°W			41.3
Silver Bell - Pima Mission	N41°W			39.6
Pima Mission - Red Mountain	N32°W			39.3
Red Mountain - Cananea	N47°W			43.0
Ray - San Manuel	N29°W			36.9

Average Values:

$$\bar{n} = \left(\sum n + \sum \frac{2n}{2} \right) / 5 = 25.6 \pm 1.0$$

$$\bar{a}_n = N72.2^\circ E \pm 4^\circ$$

$$\bar{m} = \frac{1}{5} \sum m = 40.0 \pm 3.0$$

$$\bar{a}_m = N34.8^\circ W \pm 11^\circ$$

variations in crustal thickness on them. The ultimate goal was to classify porphyry copper deposit locations by means of crustal parameters.

Data gathered by the photocell measuring of lineation data (Plates 5, 6, 7, 8, 9, 10, and 11) were subjected to a Fourier analysis which consisted of derivation of the Fourier coefficients a_p and b_p (p = harmonic number) by a Math-Pack computer program. Coefficients were derived for both rows (latitude) and columns (longitude) of photolinear intensity data.

$$\text{Normalized Fourier energy} \left(E_p = \frac{a_p^2 + b_p^2}{a_0^2 + b_0^2} \right) \text{ for selected row data}$$

in the N50°W direction was plotted as a function of harmonic number $[p \leq 1/2 (\text{number of data points}) - 1]$ to provide an energy spectrum (Figure 3). As a check, the Fourier energy was also plotted for longitude (Figure 4) and showed good agreement with latitude data (Figure 3).

Conversion of the harmonic number into harmonic spacing (perpendicular distance between lineation spacings) gives a quantitative display of fundamental spacing, e.g., for rows of data (Figure 5):

$$\text{Harmonic spacing} = 2 (\text{sample spacing}) (p + 1) \cos 50^\circ. \quad (\text{Eq. 3})$$

Comparison between harmonic spacings and distances between selected porphyry copper deposits (Table 2) shows that both the n and m distances between copper deposits are present in the Fourier data (25.0 miles and 39.5 miles). We feel that this suggests a fundamental control for both fault/fracture development and formation of porphyry copper deposits in the test area. We have not been able to determine a quantitative relationship between spacing and crustal thickness but this may be due to the paucity of crustal data in the area (Plate 12).

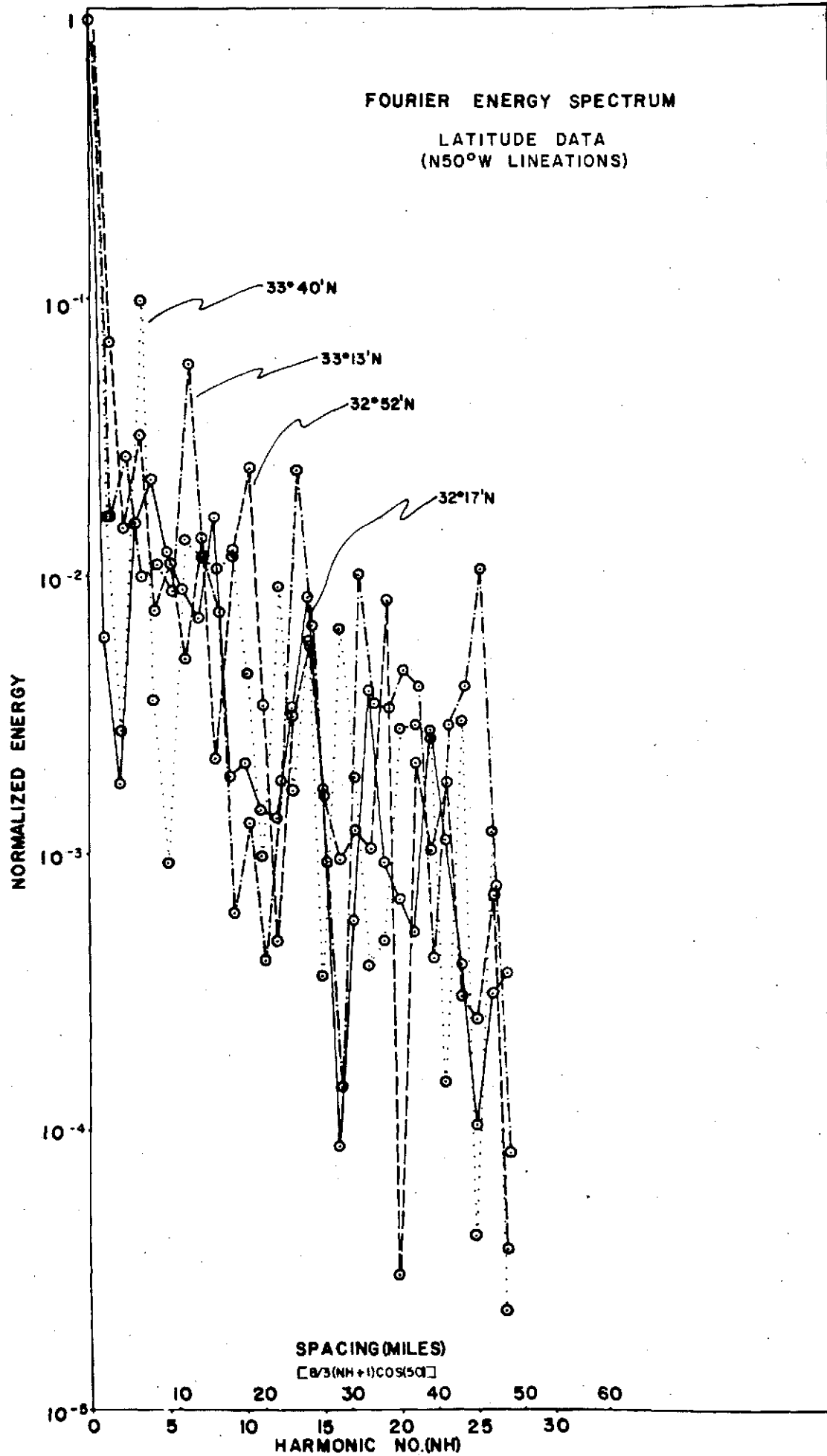


Figure 3

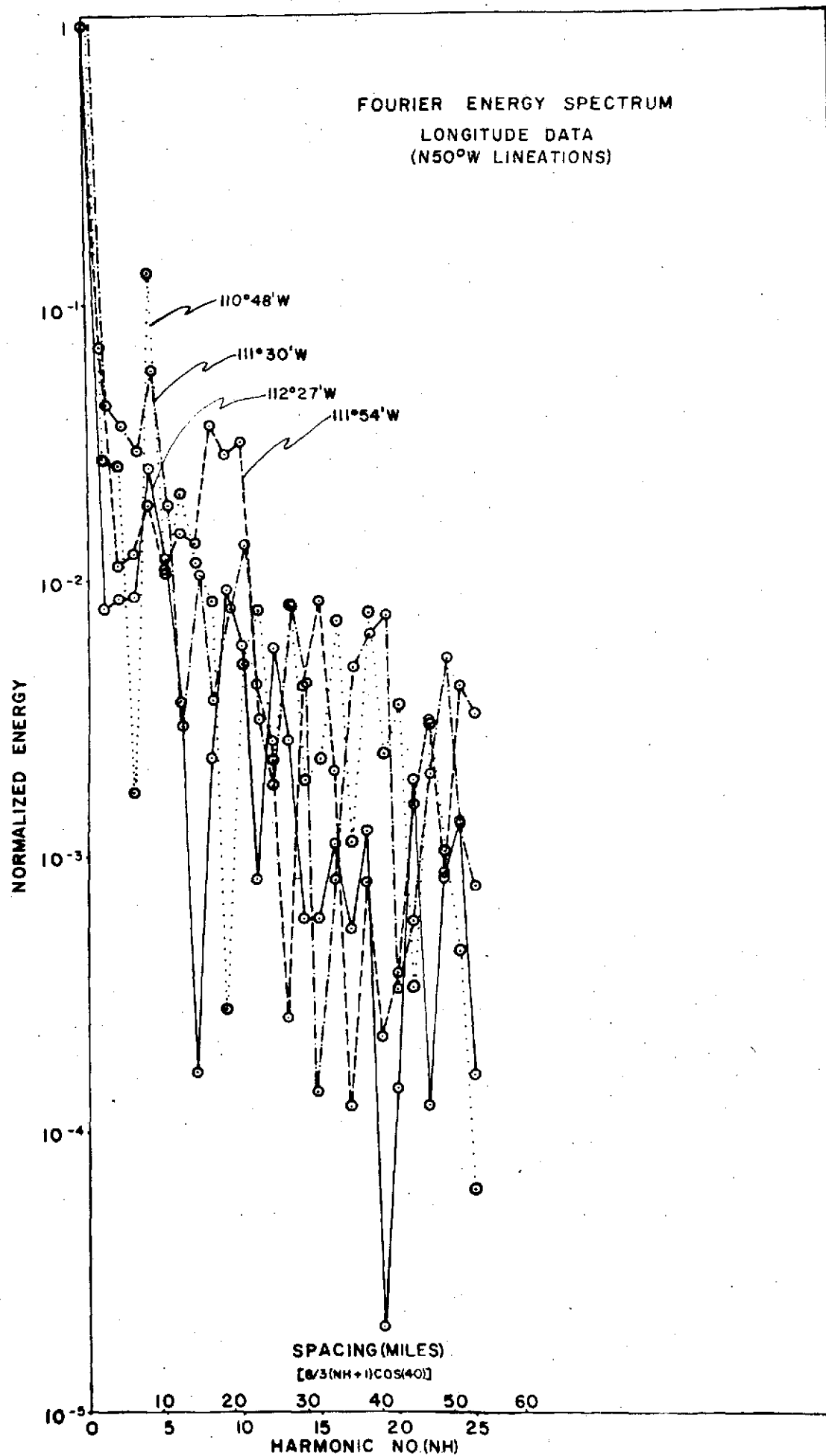


Figure 4

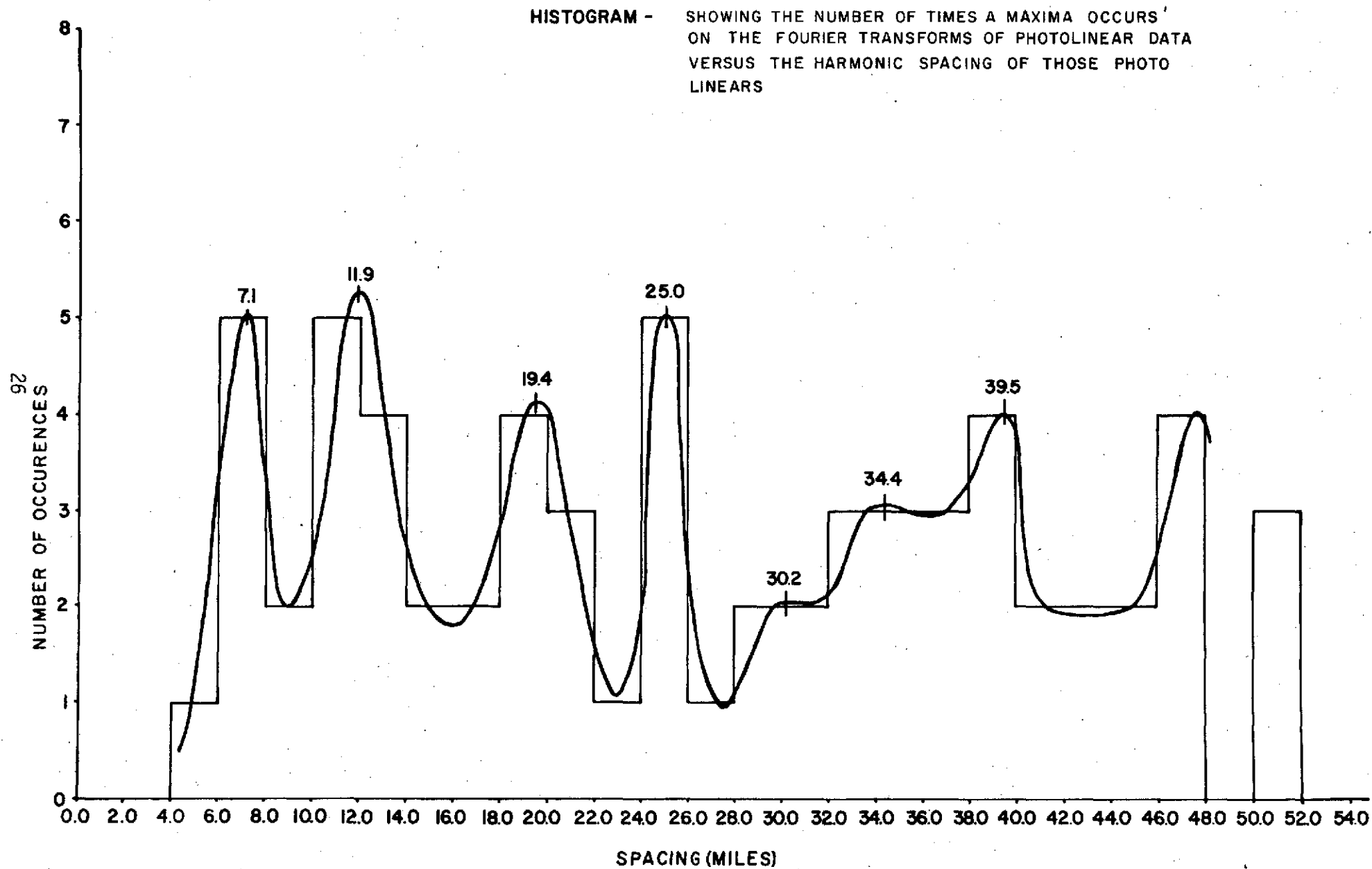


Figure 5

Additional Fourier analytical treatment of the fault intensity data is beyond the scope of this work. We feel that such treatment has a high probability of yielding significant conclusions on the nature of copper porphyry occurrences in Arizona and recommend further investigations.

COMPARISON OF ERTS IMAGERY WITH THAT BY OTHER REMOTE SENSORS

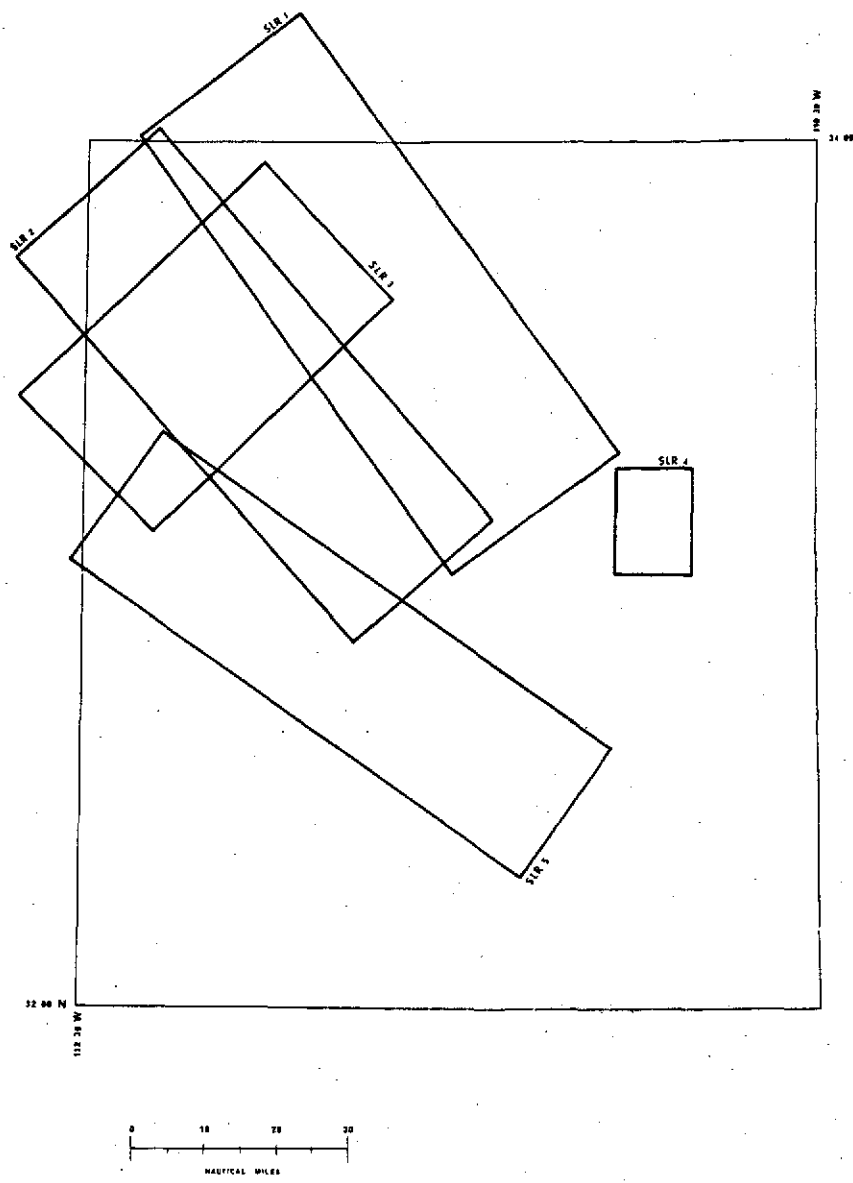
Side-Looking Airborne Radar (SLAR)

A comparison of side-looking airborne radar (SLAR) imagery from five flight lines within the ERTS test area (Figure 6) was undertaken to see if the finer ground resolution of SLAR could give additional information and detail to structural control mapped from ERTS imagery. Special emphasis was placed on intersection of fault systems at locations of known porphyries.

The low-look-angle of SLAR imagery enhances subtle geological features that are not easily determined on ERTS imagery except that of very low sun angle (high latitude or winter) ERTS imagery. The much finer ground resolution of approximately 25 feet compared to approximately 250 feet for ERTS imagery, enables more detailed mapping of lithology, bedding, joint systems and minor faults. One major advantage of SLAR imagery is the larger scale compared to ERTS (1:1,000,000 and 1:250,000) which assists in distinguishing greater geological detail, but this same detail is detrimental in interpreting the very large regional fault zones.

Flight line 5 (Figure 6) is a Northwest-Southeast SLAR traverse along Highway 84 in the vicinity of Casa Grande. The scale of the imagery is approximately 1:190,000 and it was gathered in 1971 by Aero Service utilizing the Goodyear synthetic aperture SLAR system (APQ 102). In comparing this flight line with ERTS imagery, it is interesting to note the following differences:

1. Tertiary basalts are much easier to identify on the ERTS imagery than on the SLAR imagery because of their dark colors, whereas on the SLAR imagery they appear no different in grey tone than other formations.



SIDE-LOOKING RADAR COVERAGE

Figure 6

2. Three lineation (foliation) planes can be distinguished in the Picacho Mountains on SLAR imagery. The directions of these foliation planes, which are in a Precambrian diorite porphyry, are N55°W, N65°E and North-South. These are listed in order of major-to-minor foliation planes as seen on SLAR imagery. One of the reasons that N55°W foliation plane is so dominant on SLAR imagery is that it is nearly orthogonal to the scan line which, in turn, is perpendicular to the direction of flight. An examination of ERTS imagery (scale 1:250,000) for similar foliation planes shows that only the N65°E lineation is clearly defined and the others are barely recognizable and would not be mapped without the aid of SLAR imagery. ERTS imagery dates, with the exception of one frame (1065-17204), are November 1 through November 22, 1972. It should be noted that the sun elevation angle for these dates is 29° to 39° with an azimuth of 148° to 154°. Lineations at approximately right angles to this are more easily detected which explains why the N65°E foliation plane is the most noticeable. Similar reasoning holds for SLAR in that different flight azimuths will delineate or enhance different foliation planes. It is estimated that the SLAR illumination angle of the Picacho Mountains is approximately 35°.

SLAR imagery from flight line 4 is also from the Goodyear System (scale of 1:100,000) and shows a number of fault systems and foliation planes that intersect the Ray Mine area. However, the regional fault systems associated with the Ray Mine are quite adequately displayed on the 1:250,000 enlarged ERTS coverage.

SLAR imagery from flight lines 1, 2, and 3 was furnished by SAC Air Force Systems Command utilizing a Goodyear Aerospace SLAR system. This high-resolution imagery enabled a number of fault systems to be traced through the alluvial areas, and in some cases detected secondary foliation planes that were not visible in the ERTS imagery.

Deformed rocks have diverse origins and frequently have long and complicated histories of development. Rock fabrics (jointing, foliation, and lineations) in part record the evolution of lithologic units. To properly interpret mineralization a thorough knowledge of foliations present is essential.

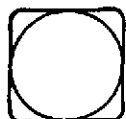
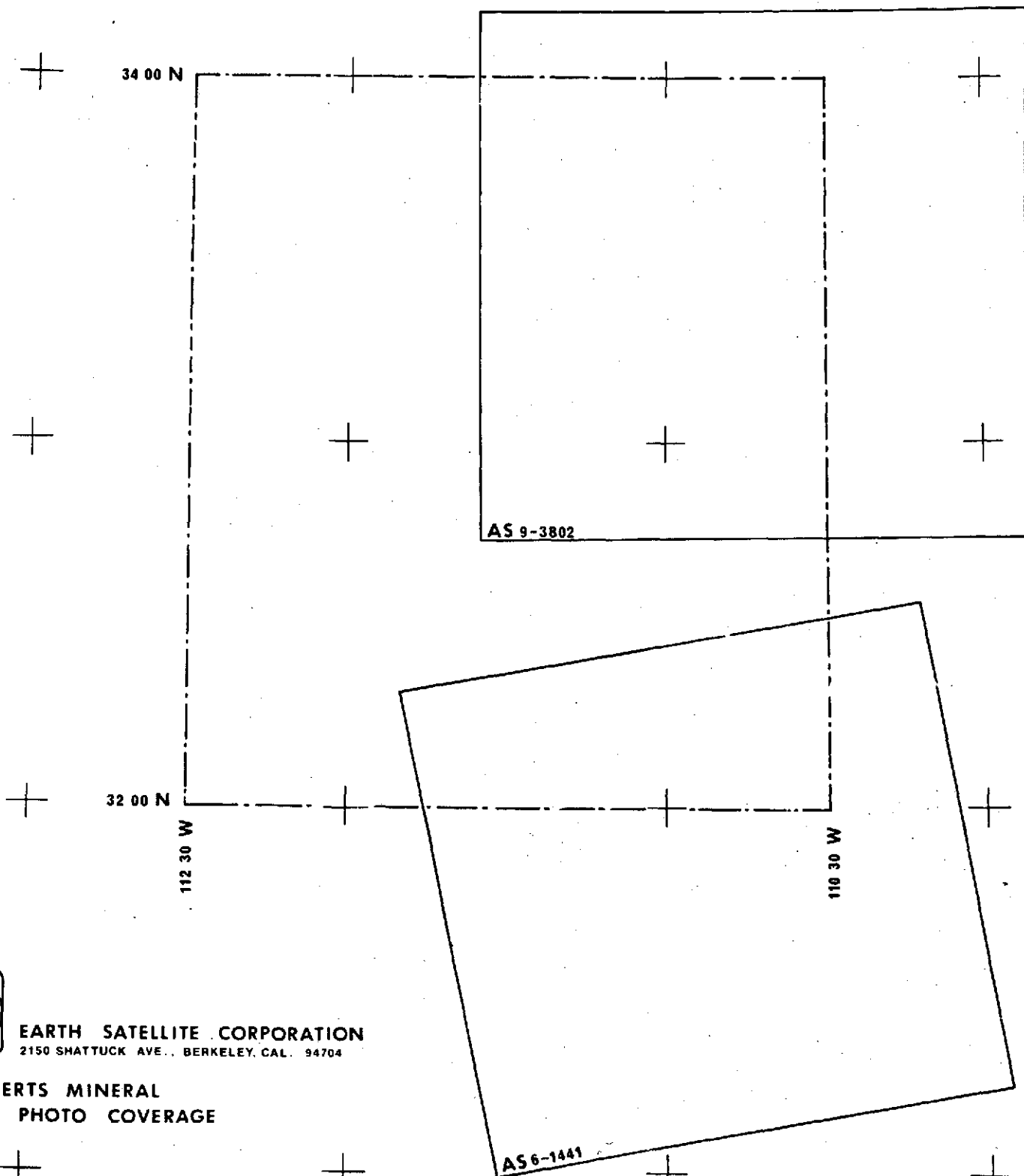
Because ERTS ground spatial resolution of approximately 250 feet does not permit adequate differentiation of lineations into faults, joints and foliations, ERTS imagery is not suitable for detailed fabric studies. When ERTS imagery is used in conjunction with finer resolution sensors, i.e., Apollo, Gemini and Skylab photography and SLAR imagery, it is frequently possible to interpret useful fabric data.

Apollo Photography

Figure 7 displays Apollo photography coverage in relation to the ERTS study area. A black-and-white print (scale 1:932,000) of an Apollo photograph (AS9-3802) was previously interpreted for lineations which were divided into four well-developed directional systems: (1) East-West, (2) Northeast, (3) North-Northwest, and (4) North-Northeast, with emphasis on through-going structures and structures related to copper porphyries. See Figure 8 for the Apollo lineation study.

Comparison between the Apollo and ERTS interpretations of the same area (which were done by different interpreters) shows a remarkable agreement in both location and trend of linear features. As might be expected, the finer resolution Apollo photo enables greater detail to be mapped than is possible on the ERTS imagery, especially in alluvium-covered areas east and southeast of Phoenix. This higher resolution also enables mapping of finely developed jointing planes, and better discrimination between lithology, jointing systems, bedding and faults. In addition, the higher resolution enables tracing of fracture systems for greater distances.

This is especially noticeable in the North-South and East-West fault trends of the Apollo photos. The East-West trends have greater curvature



EARTH SATELLITE CORPORATION
2150 SHATTUCK AVE., BERKELEY, CAL. 94704

**C-O61 ERTS MINERAL
APOLLO PHOTO COVERAGE**

Figure 7

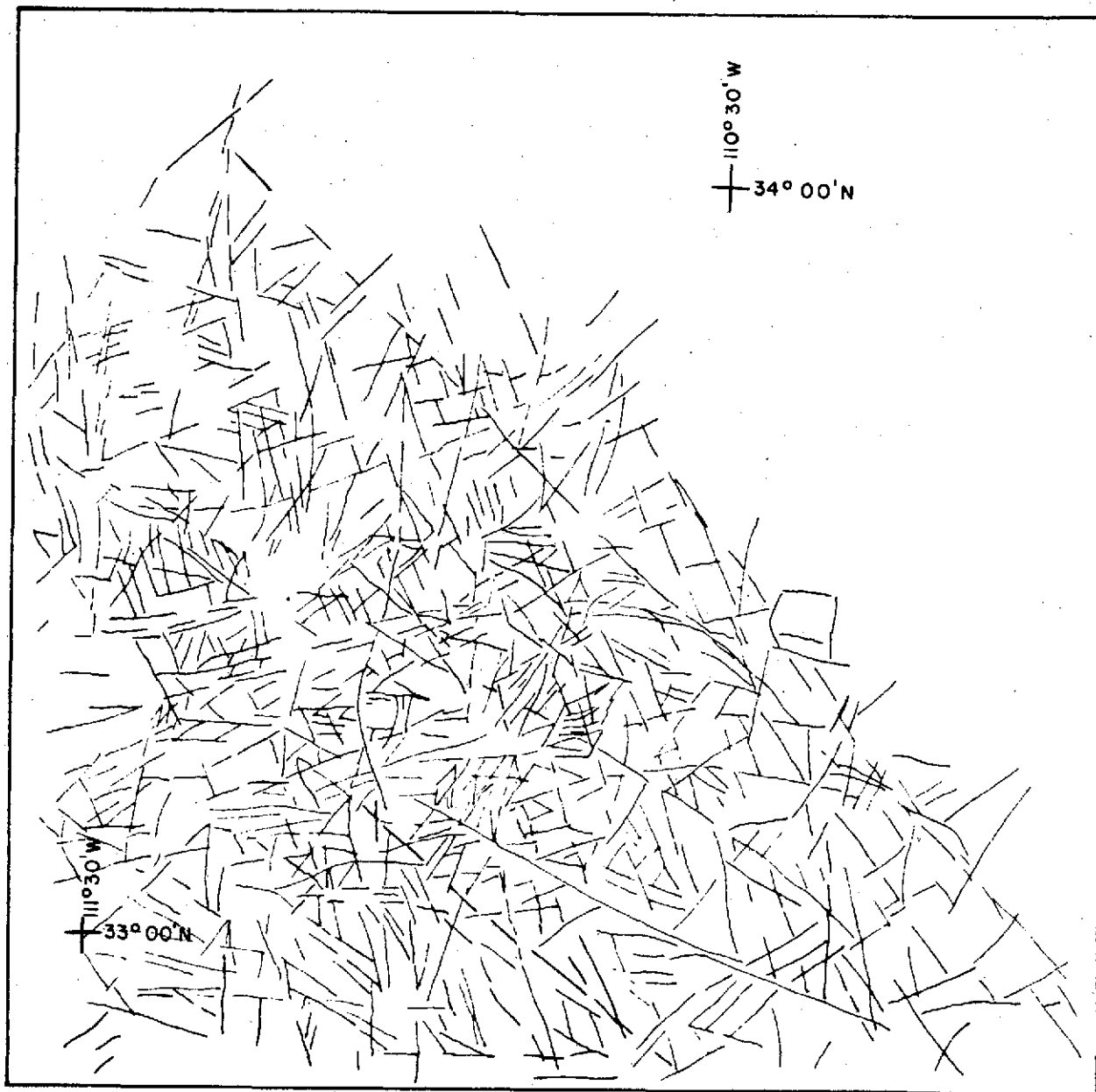


PHOTO STRUCTURAL RAW DATA



APOLLO PHOTO NO. AS9-3802

SCALE 1:932,000

Figure 8

on the Apollo interpretation than the East-West trends (Figure 9) shown on the ERTS interpretation (Plate 4). Examination by a third interpreter was done to confirm this because the two original interpreters had different styles in that one interpreted more through-going structures than the other.

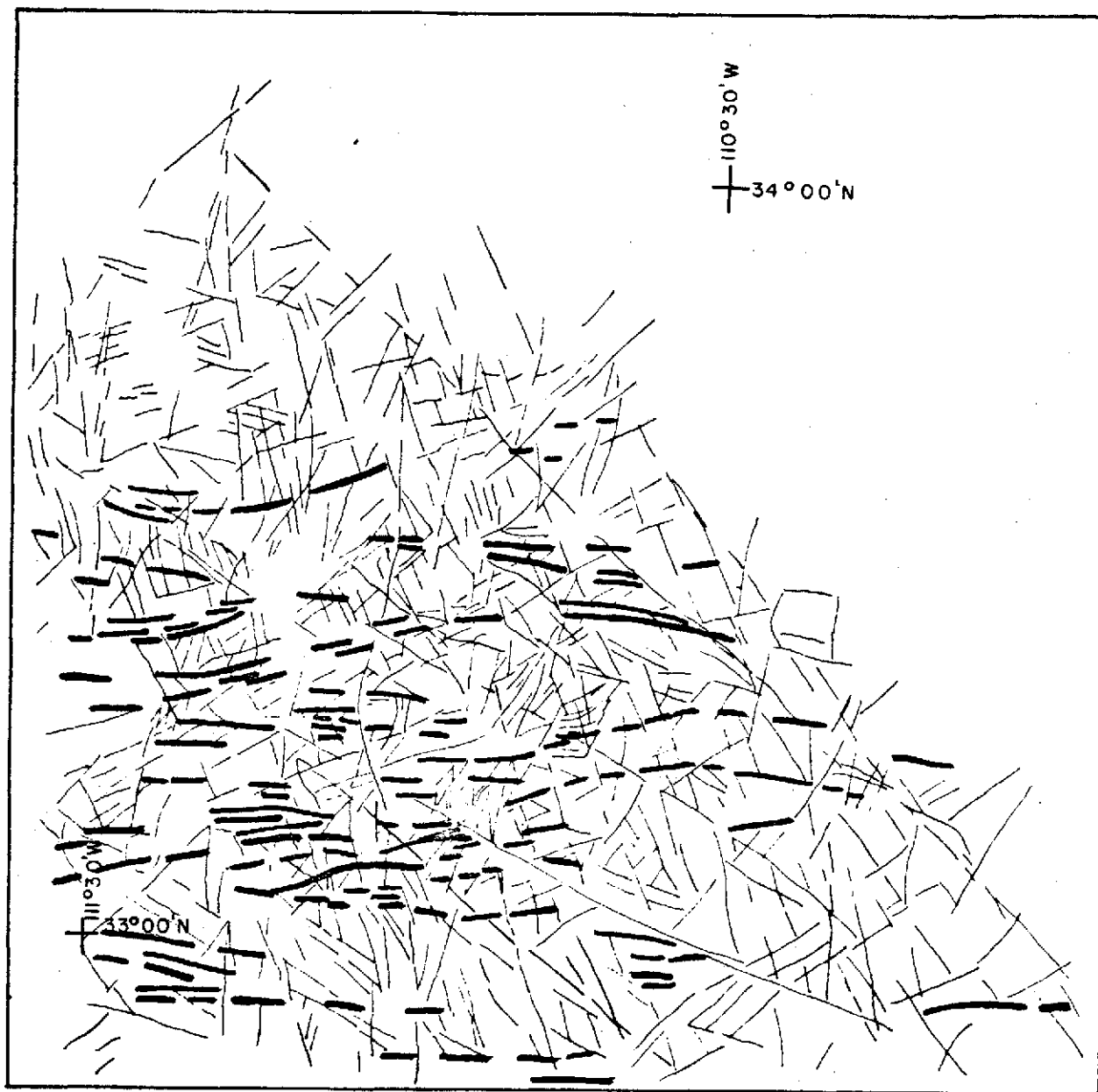
A color Apollo print (#AS6-1441) at a scale of approximately 1:932,000 was examined for comparison to an ERTS color composite transparency (scale 1:1,000,000) (1085-17332-4, 5, and 7; 16 Oct. 1972) of an area immediately west and southwest of Tucson. Following is an itemized list of significant differences:

1. Quaternary basalts are more easily identified on the ERTS imagery.
2. Bedding planes in Laramide sandstones can be detected in the Apollo photography but not on the ERTS.
3. A greater range of hues is present in the ERTS color composite than the Apollo color print. This may be due to the fact that the 35mm negative used for making the Apollo print was third or fourth generation.

In summary, it is important to mention that although Apollo photography has slightly better resolution for detecting jointing and bedding planes, the systematic ERTS 18-day cycle makes it a better overall tool for obtaining orbital coverage for geological purposes. If the RBV with its finer spatial resolution were functioning, it might have assisted in the definition of bedding, jointing and contacts. Apollo photos are useful for determination of the nature of lineations mapped on ERTS imagery.

Colored Aerial Photography

Natural color and color infrared photography from mission 72-102 (U-2) was interpreted (at a scale of 1:130,000) to determine hydrothermal alteration at locations as seen in Plate 13.



EMPHASIZE EW STRUCTURES



APOLLO PHOTO NO. AS9-3802

SCALE 1:932,000

Figure 9

Known alteration zones related to porphyry copper deposits at Silver Bell and Ajo are characterized on color infrared photography from U-2 aircraft by exceptionally fine-grained drainage patterns and a distinctive light-to-dark, yellow-brown color.

Four ERTS color composites at a scale of 1:1,000,000 were examined to determine if hydrothermal alteration zones are detectable on them. Areas that show color contrasts that may be due to alteration are shown on Plate 13 for both the ERTS and the U-2 imagery.

The known areas at Silver Bell and Ajo cause color anomalies on ERTS imagery (under 10x magnification) but lack of sufficient spatial resolution hinders identification of drainage textures. Examination of black-and-white ERTS prints (bands 4 through 7) for these areas does not reveal unique tone anomalies attributable to alteration.

Areas on Plate 13 indicated as "possible" and "barely possible" hydrothermal locations from U-2 photography can be identified on ERTS color composites but are locations that, in most cases, would not have been independently selected on the ERTS imagery.

Detection of hydrothermal alterations is a difficult task on large-scale (1:24,000) natural color photography, even where alteration results in maximum color contrast with "country rock" in arid areas with minimum vegetation.

We believe that the very subtle hue changes associated with hydrothermal alteration are difficult to recognize on small-scale ERTS imagery. The many reddish and reddish-brown colors present are probably due to vegetation rather than directly to rock types, and there is as yet no basis for ascribing such vegetation variations indirectly to (hydrothermal) compositional anomaly via the geobotanical effect. Small-scale U-2 photography and ERTS imagery were

interpreted for possible hue variations that might reflect: (1) widespread feldspar alteration (to clay minerals) which usually appear as a lighter-toned outcrop area compared with unaltered outcrops of the same rock type(s), (2) iron staining that appears as a red or pink hue on outcrops or on shallow alluvium overlying bedrock alteration zones and, most importantly, (3) very fine local drainage nets, vegetative cover and outcrop data that aids an experienced interpreter to decide which combination of effects could indicate alteration zones. Use of these three techniques is difficult and, in the case of item (3), beyond the capability of ERTS-MSS data.

Aeromagnetics

Interpretation of the Residual Aeromagnetic Map of Arizona (1970) for linear trends resulting from regional faulting of the basement is presented in Plate 14.

Data for the magnetic map were collected at elevations of about 6,000 feet above terrain along North-South traverses spaced three miles apart. This causes anomalies due to sharp basement discontinuities, e.g., faults, to appear as broad features on the map (over three miles wide). Thus, locations of faults interpreted on Plate 14 (from aeromagnetics) and of those shown on ERTS imagery interpretations (Plates 3 and 4) do not necessarily coincide. However, ERTS (Plate 4) and aeromagnetic interpretations are in general agreement in showing major Northeast and Northwest trending faults.

Systems "A" (N40°E to N50°E) and "B" (N50°W) noted on the ERTS lineation study (Plate 4) are dominant in the magnetic interpretation, especially in the southern three-fourths of the test area.

To perform further comparisons between ERTS and aeromagnetic data, it is recommended that the aeromagnetic data be processed by Fourier analysis.

All of the other systems noted in the ERTS study are represented in the magnetic trends but are notably subordinate to systems "A" and "B." Systems "G" (N75°W) and "H" (East-West) are well represented in the northern part of the test area by magnetic trends and the other systems of the ERTS lineation study ("C," "D," "E," and "F") are represented by occasional faults and trends on the magnetic interpretation.

System "E" (North-South), one of the strongest on the ERTS lineation survey, is represented by only one fault on the magnetic interpretation within the test area and appears as a strong magnetic trend in the north-western part of the test area. This suggests that this direction represents an extensional system of features with very shallow depths of faulting.

Study of the aeromagnetic map and porphyry locations shows that copper occurrences are generally located on flanks of magnetic lows but there is no preferred orientation of magnetic faults or trends associated with the porphyries nor do they occur at intersections of features noted in the interpretation.

FIELD CHECK

During the week of March 5 through 7, 1973 two Earth Satellite geologists visited the test site to conduct ground investigations of tectonic features and hydrothermal altered areas that were observed on the U-2 and ERTS imagery. Whenever possible, observations were made both at the exact location of the feature being investigated and from nearby hills and mountains in an effort to see the control of regional faults on topography.

Geological maps of the Salt River Mountains, south of Phoenix, show that the range is composed of Precambrian granitic gneiss with primary foliation oriented Northeast that exerts control on topographic expression. This foliation is easily mapped on ERTS imagery. A Laramide granitic intrusion into Precambrian gneiss, shown on the map, is not recognized on the ERTS imagery. On ERTS imagery the intrusion is interpreted as a wide fault zone trending Northwest. Some major features such as the Gila River-Salt River zone that are very apparent on the ERTS mosaic and are discussed under the regional tectonics section cannot be identified. This demonstrates the importance of ERTS mosaics at small scales for studying regional tectonics.

A field trip to the Sacaton, Posten Butte and Ray areas was made in an effort to trace, on the ground, a lineation system connecting these areas that is observed on ERTS and Apollo imagery. The trip was unsuccessful because the lineation is obscured on the ground by topographic trends across it which are stronger than any topographic or geologic features related to it. This is a good area to demonstrate how in ERTS imagery long lineations (10 miles or longer), that are partially covered by large sections of alluvial cover and crossed by topographic features related to more recent tectonic activity, can be traced and joined.

Two of the prospective areas, discussed on pages 15 and 20, were visited to see if features observed on ERTS imagery could be identified in the field. These areas were the region around Castle Dome, Cactus and Bluebird mines (Plate 3) and an area further to the east (approximately 6 miles) located around Miami-Inspiration (Figure 2). As was the case in Sacaton, Posten Butte and Ray, lineations observed on ERTS imagery are not easily identified in the field.

One of the criteria used in selecting these prospective areas was the spatial correlation of high intensity contours from Plates 7 and 8 (intersection location of $N70^{\circ}E$ and N-S lineations), that can best be seen from higher altitudes such as satellite imagery. Another criteria used for the selection of these prospective areas was aeromagnetics anomalies which cannot be observed directly in the field. For these reasons the other prospective areas shown on Plate 3 and Figure 2 were not visited.

SUMMARY AND CONCLUSIONS

Our investigation shows that ERTS imagery is a useful tool for evaluation of regional structural relationships and reconnaissance definition of mineral exploration targets. Attempts to extend the use of ERTS imagery to location and definition of specific areas for exploration (less than 15 square kilometers) had only limited success.

In addition to the objectives listed and the work plan presented in our proposal, we performed an experiment to test the hypothesis that occurrence of porphyry copper deposits is related to spacing between parallel fault trends that in turn may be related to crustal properties. Preliminary results of Fourier analysis of data for faults trending N50°W show fundamental spacings between Fourier energy maximum that can be related to distances between copper deposits. We feel that the method shows promise and recommend further investigations.

Objectives of the investigation, as defined in our proposal, were realized to varying degrees and are discussed below.

The first objective of our work, to establish the usefulness of ERTS imagery in determining spatial relationships between copper deposits, Laramide porphyry intrusions and regional tectonic features (principally fault trends), was met. Regional Northeast trending lineations observed on ERTS imagery are the manifestation of fault trends controlling copper deposits, especially in the Globe-Miami-Ray area (Plate 3). Northwest lineation trends are interpreted as secondary controls for mineral emplacement. Both Northeast and Northwest systems are considered as manifestations of zones of weakness that served as loci

for mantle-derived magmas to intrude the crust during the Laramide orogeny. Preliminary Fourier analysis of ERTS lineation data indicates that it is a useful tool for recognition of spacings of fault trends.

A factor that is not completely understood, but plays an important role in ore genesis, is tectonic style, which is used here to define tectonic units. We feel that the nature of the boundaries of these units and relationships within the units to boundaries may be explained by stress systems associated with the San Andreas Fault system. These systems were probably operative during Laramide igneous activity and exerted significant controls on genesis of copper deposits.

Results of attempts to interpret the tectonic framework, observed on ERTS imagery, using concepts of the "New Global Tectonics," projected to the continental environment of the test area, were inconclusive. All of our hypotheses involving the use of spreading centers and transform faults under the continent have weaknesses and contradictions that do not permit rigorous treatment.

Our studies of ERTS imagery to recognize rejuvenated structures and their association with mineralization and igneous intrusive activity were not successful. The Northeast and Northwest trends of faults and fractures that apparently exert control on mineralization are readily recognized on ERTS imagery but relationships and interactions of these systems with pre-existing trends, if present, are not clear. We do believe that North-Northeast and East-West lineation systems are the youngest in the area because of the sharpness and narrowness of their traces but cannot definitely ascertain their relationship to Laramide tectonic features.

Our goal to determine configuration of and relationships between crustal blocks, concentration of younger plutons, and location and extent of fracture zones was met and is exemplified by the nine tectonic units which we define. Younger volcanic rocks are primarily present in units III and VII and older volcanic rocks are dominant in V and VI. The tectonic setting of the area can be explained by a stress system related to compressional forces associated with the San Andreas Fault. In this system, tectonic unit boundaries are interpreted as decoupling zones and faults within units are visualized as the result of reorientations of stress directions in the manner presented by Moody and Hill (1956).

Short-term objectives of our work to evaluate and compare ERTS imagery with U-2 and Apollo photos, SLAR and aeromagnetic data, were accomplished.

The long-term goal to determine how ERTS imagery can be used for regional tectonic analyses of areas which have not been studied as extensively as the test area is promising. Techniques of ERTS imagery interpretation devised for the test area can be used in areas of the world where little or no geological data are available. Tectonic maps of such areas can be readily compiled for mineral exploration use and for other purposes existing tectonic maps can be updated. This can best be accomplished by using imagery at scales of 1:1,000,000, 1:500,000 and 1:250,000.

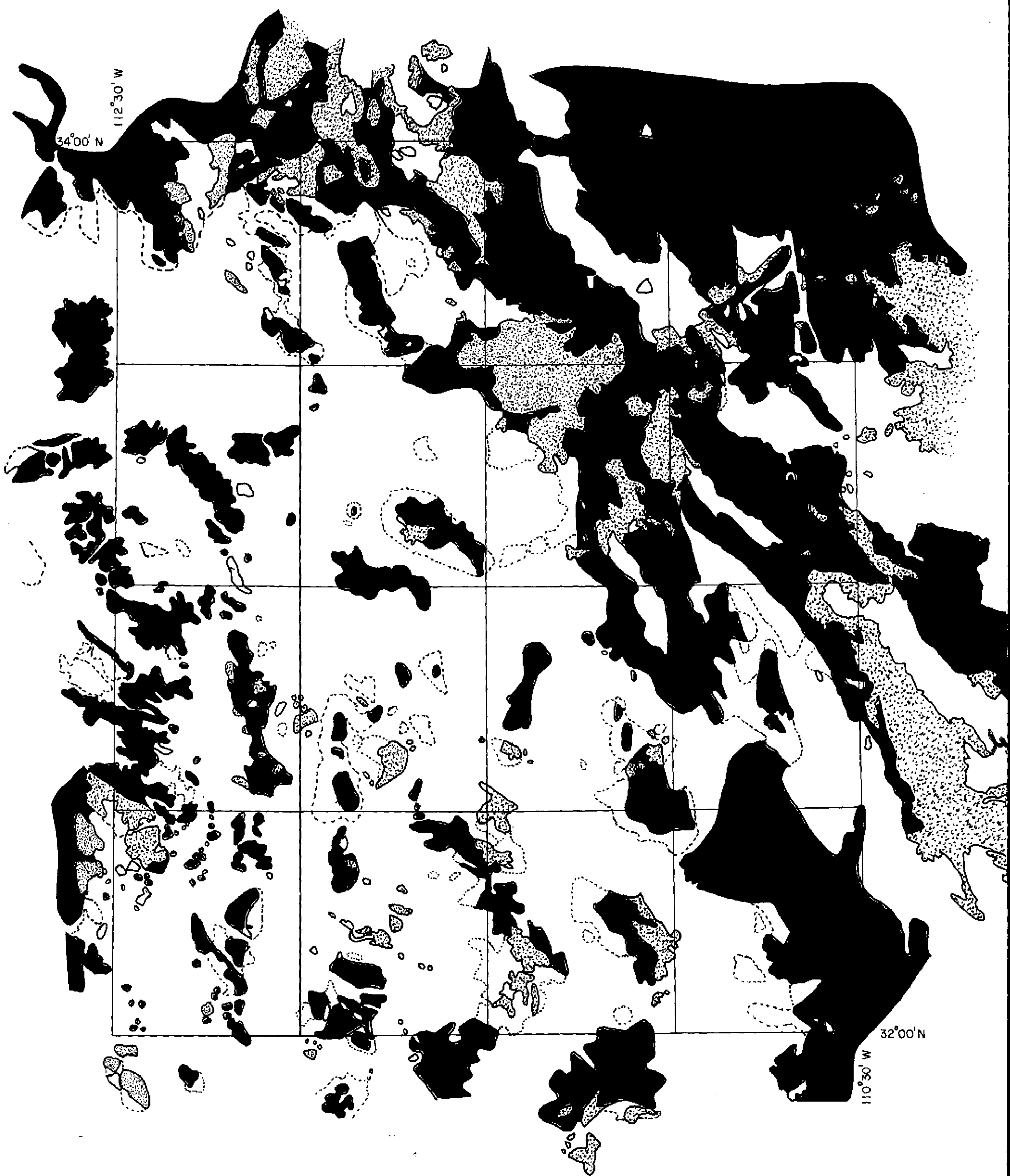
Our work demonstrates that the tectonic map approach can reveal a wealth of geological data, especially in arid and semi-arid climates. Further studies should be directed toward similar applications in humid and tropical areas.

The use of ERTS imagery in exploration for mineral deposits by mapping structural trends and by detection of indicators

(combination of ERTS data with SLAR, aeromagnetic and gravity information) for identifying target areas will probably be more valuable in areas of the world that are less extensively explored than is the test area of this study. Interpretation of ERTS imagery prior to localized airborne remote sensing surveys and ground investigation can direct explorationists to favorable target areas and promises considerable saving of time and money.

REFERENCES CITED

- Billingsley, P. and A. Locke, 1941, Structure of Ore Districts in the Continental Framework, American Institute of Mining and Metallurgical Engineers Transactions, v. 144, p. 9-64
- Blanchet, P. H., 1967, Personal communication
- Cloos, H., 1939, Hebung-Spaltung-Vulkanismus, Geologische Rundschau, v. 30, p. 401-527, 637-640
- Cohee, G. V. (Chairman), 1962, Tectonic Map of the United States (exclusive of Alaska and Hawaii) (scale 1:1,000,000), U.S. Geological Survey and the American Association of Petroleum Geologists
- Mayo, E. B., 1958, Lineament Tectonics and Some Ore Districts of the Southwest, Mining Engineering, v. 10, p. 1169-1175
- Moody, J. D. and M. J. Hill, 1956, Wrench-Fault Tectonics, Geological Society of America Bulletin, v. 67, p. 1207-1246
- Sauck, W. A. and J. S. Sumner, 1970, Residual Aeromagnetic Map of Arizona, Department of Geological Sciences, University of Arizona, Tucson, Arizona
- Schmitt, H. A., 1966, The Porphyry Copper Deposits in Their Regional Setting, In Geology of the Porphyry Copper Deposits, Southwestern North America, Titley, S. R. and C. L. Hicks, editors, University of Arizona Press, Tucson, Arizona
- Stratton, J. A., 1941, Electromagnetic Theory, McGraw-Hill, New York and London, 615 p
- U.S. Department of Commerce, 1965, Operational Navigation Chart (scale 1:1,000,000) ONC, G-19, National Ocean Survey, Washington, D.C.
- Warren, D. H., 1969, A Seismic Refraction Survey of Crustal Structure in Central Arizona, Geological Society of America Bulletin, v. 80, p. 257-282
- Wertz, J. B., 1970, The Texas Lineament and Its Economic Significance in Southwest Arizona, Economic Geology, v. 65, p. 166-181
- Wilson, E. D., R. T. Moore and J. R. Cooper, 1969, Geologic Map of Arizona (scale 1:500,000), Arizona Bureau of Mines and the U.S. Geological Survey
- Woolard, G. P. (Chairman) and H. R. Joesting (Coordinator), 1964, Bouguer Gravity Anomaly Map of the United States (exclusive of Alaska and Hawaii) (scale 1:2,500,000), American Geophysical Union and the U.S. Geological Survey



EXPLANATION

OUTCROP MAP AS SEEN ON ERTS-MSS MOSAIC

- PRETERTIARY ROCKS CORRELATED WITH ERTS-DERIVED OUTCROP DATA.
- POSSIBLE AREA OF OUTCROP OR THIN COVER REVEALED ON ERTS/MSS IMAGERY.
- TERTIARY / QUATERNARY IGNEOUS ROCKS, TRACED FROM EXISTING GEOLOGIC MAPS AND PARTIALLY CORRECTED TO ERTS MAP BASE.

GEOLOGY DATA FROM GEOLOGIC MAP OF ARIZONA (1969 Ed.)

ERTS-1 ARIZONA MINERAL

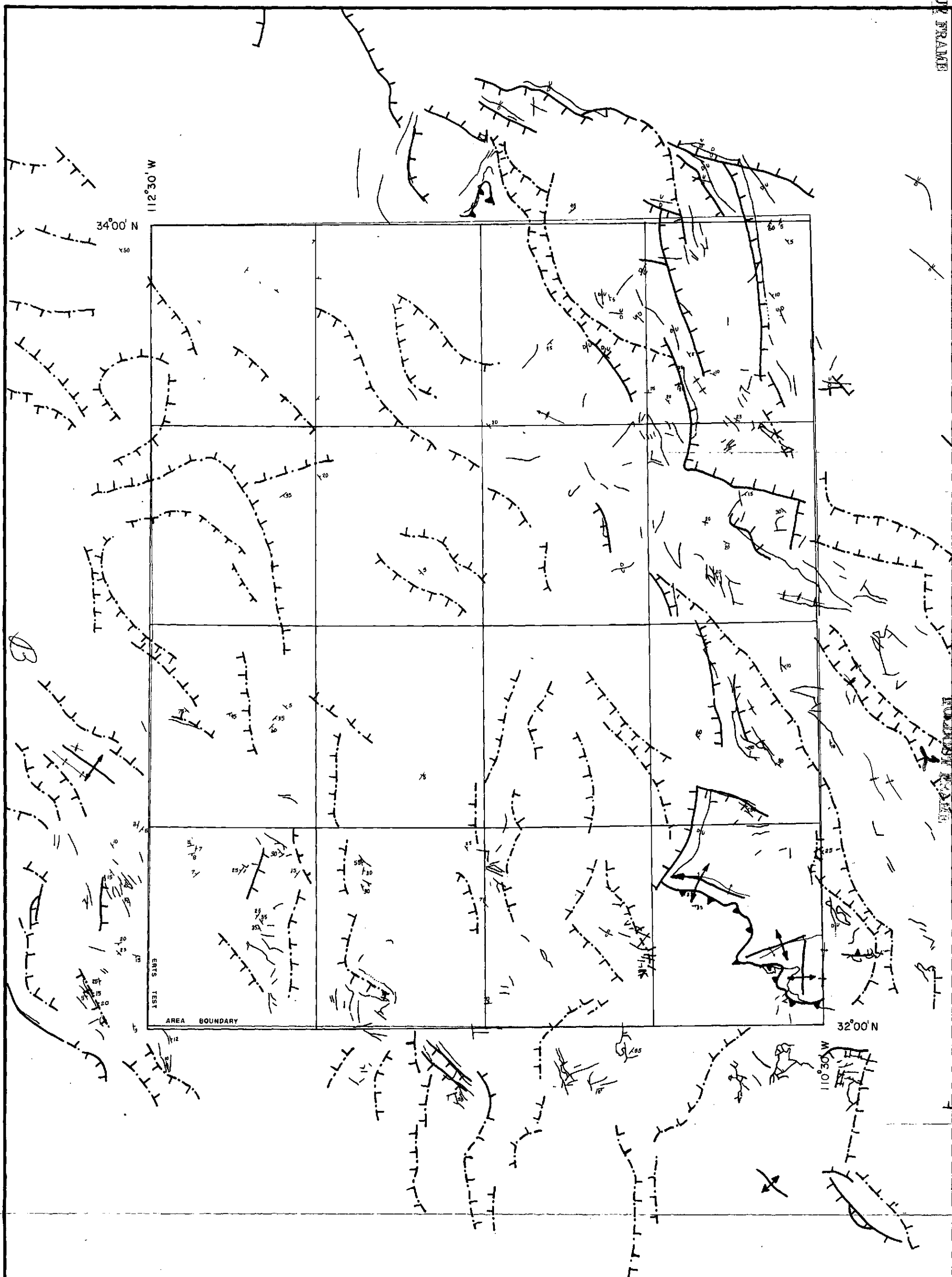
For: NASA ERTS CONTRACT No. G-061

EARTH SATELLITE CORP.

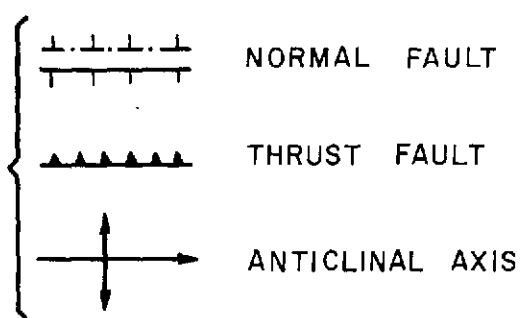
2150 SHATTUCK AVE., BERKELEY, CAL. 94704

DATE: AUG 20, 1973	PLATE No. 1	SCALE: 1:1,000,000	DRN. BY: JLW
-----------------------	----------------	-----------------------	-----------------

EarthSat



EXPLANATION



Taken from Tectonic Map of the United States U.S.G.S. 1962 Ed. Scale: 1:2,500,000 Conic projection

Taken from Geologic Map of Arizona (1:500,000) The Arizona Bureau of Mines/U.S.G.S. 1969 Ed. (Lambert conformal conic projection/standard parallels 33° and 45°)

SYMBOL	EXPLANATION
— —	NORMAL FAULT
—▲—	THRUST FAULT
—+—	SYNCLINE
—x—	ANTICLINE
—/—	STRIKE & DIP

STRUCTURE MAP (FAULTING AND FOLDING)

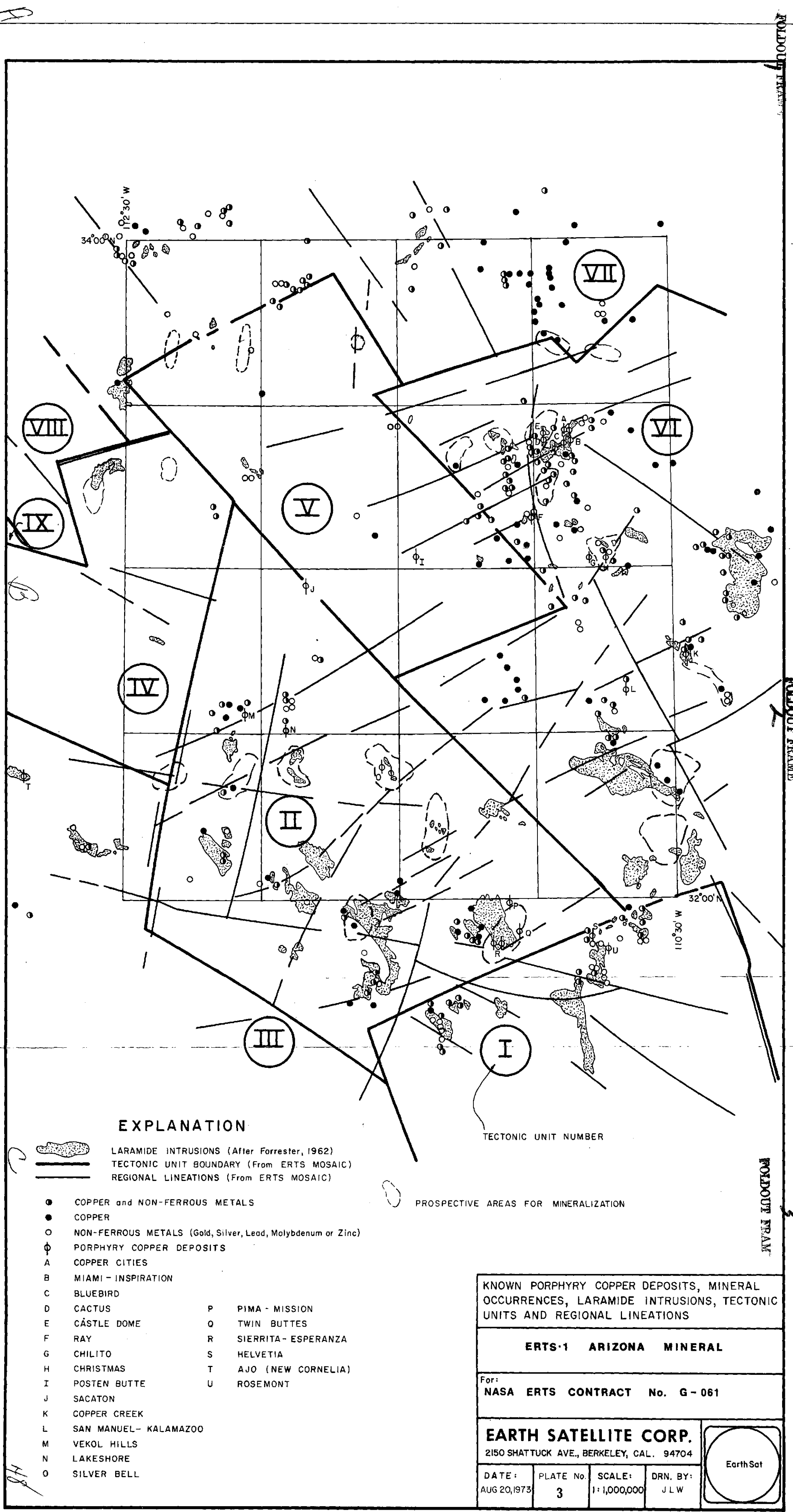
ERTS-1 ARIZONA MINERAL

For: **NASA ERTS CONTRACT No. G-061**

EARTH SATELLITE CORP.
2150 SHATTUCK AVE., BERKELEY, CAL. 94704

DATE: AUG 20, 1973	PLATE No. 2	SCALE: 1:1,000,000	DRN. BY: JLW
-----------------------	----------------	-----------------------	-----------------

EarthSat



EXPLANATION

- LARAMIDE INTRUSIONS (After Forrester, 1962)
- TECTONIC UNIT BOUNDARY (From ERTS MOSAIC)
- REGIONAL LINEATIONS (From ERTS MOSAIC)

- COPPER and NON-FERROUS METALS
- COPPER
- NON-FERROUS METALS (Gold, Silver, Lead, Molybdenum or Zinc)
- ⊕ PORPHYRY COPPER DEPOSITS
- A COPPER CITIES
- B MIAMI - INSPIRATION
- C BLUEBIRD
- D CACTUS
- E CASTLE DOME
- F RAY
- G CHILITO
- H CHRISTMAS
- I POSTEN BUTTE
- J SACATON
- K COPPER CREEK
- L SAN MANUEL - KALAMAZOO
- M VEKOL HILLS
- N LAKESHORE
- O SILVER BELL
- P PIMA - MISSION
- Q TWIN BUTTES
- R SIERRITA - ESPERANZA
- S HELVETIA
- T AJO (NEW CORNELIA)
- U ROSEMONT

TECTONIC UNIT NUMBER

PROSPECTIVE AREAS FOR MINERALIZATION

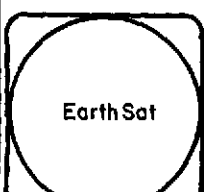
KNOWN PORPHYRY COPPER DEPOSITS, MINERAL OCCURRENCES, LARAMIDE INTRUSIONS, TECTONIC UNITS AND REGIONAL LINEATIONS

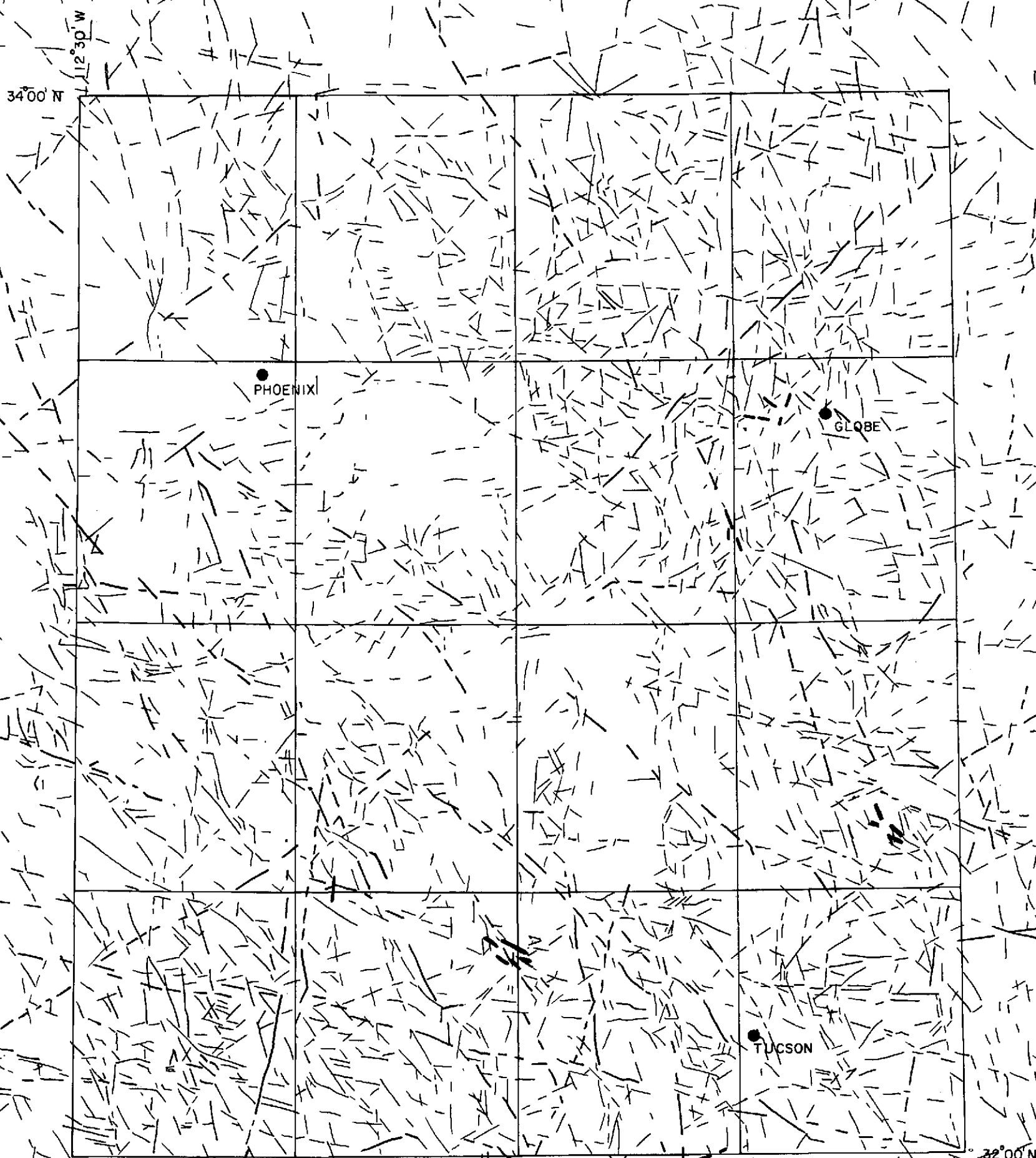
ERTS-1 ARIZONA MINERAL

For: NASA ERTS CONTRACT No. G-061

EARTH SATELLITE CORP.
2150 SHATTUCK AVE., BERKELEY, CAL. 94704

DATE: AUG 20, 1973
PLATE No. 3
SCALE: 1:1,000,000
DRN. BY: J.L.W.





EXPLANATION

COMBINED AND SIMPLIFIED INTERPRETATION OF ERTS MSS MOSAIC FOR GEOLOGIC STRUCTURE.

- MINOR LINEATIONS
- MAJOR LINEATIONS
- PREVIOUSLY GROUND MAPPED FAULTS AT PORPHYRY COPPER LOCALITIES

ERTS-1 ARIZONA MINERAL

For:
NASA ERTS CONTRACT No. C-061

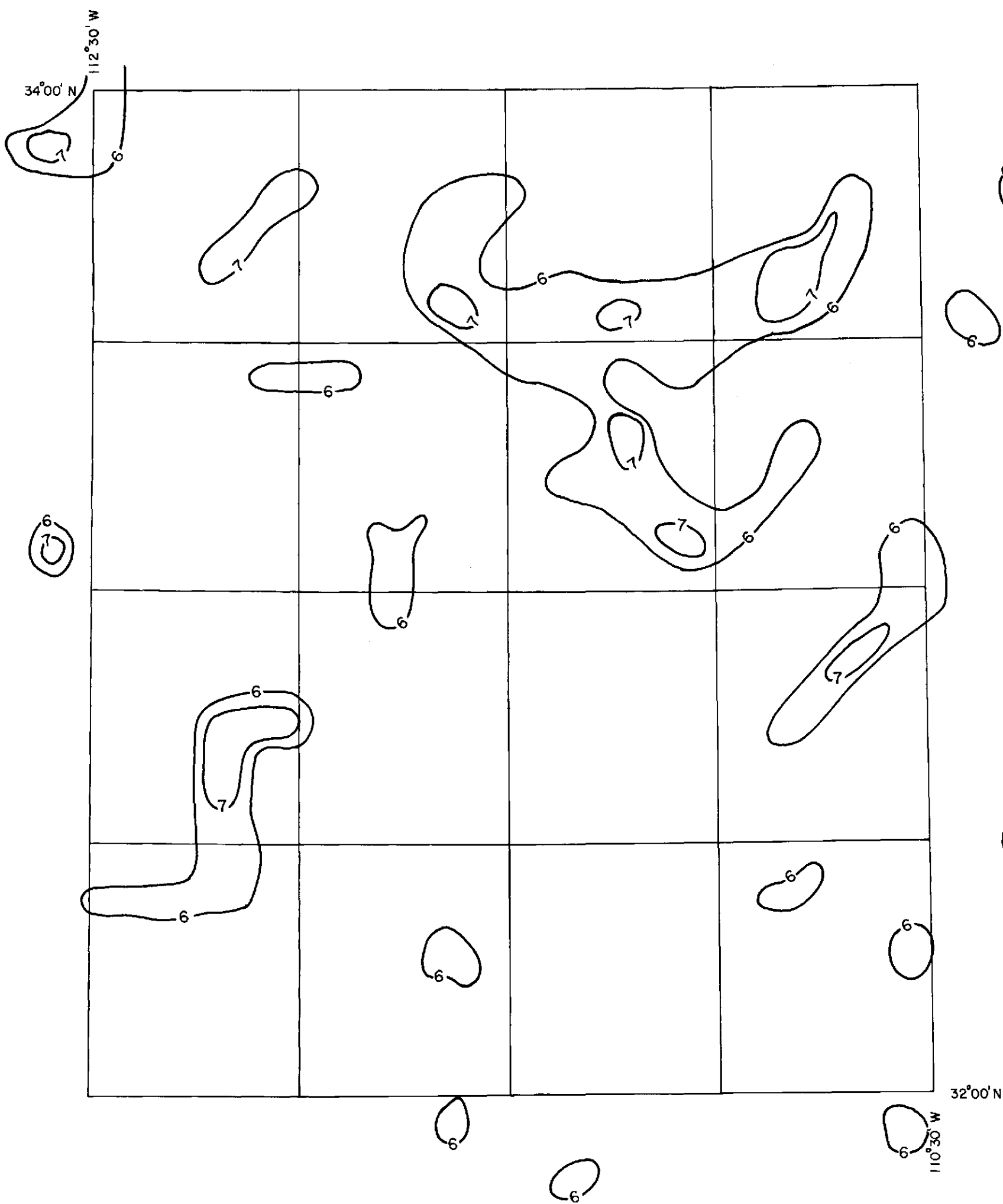
EARTH SATELLITE CORP.
2150 SHATTUCK AVE., BERKELEY, CAL. 94704

DATE: AUG 20, 1973	PLATE No 4	SCALE: 1:1,000,000	DRN. BY: J.L.W.
-----------------------	---------------	-----------------------	--------------------

EarthSat

FOLDOUT FRAME

N45°E



FOLDOUT FRAME

Contour Intensity Equivalents
 6 (Meter Units) = 0.5 Foot Candle
 7 (Meter Units) = 1.0 Foot Candle
 CONTOUR INTERVAL ONE LUNA PRO LIGHT METER UNIT

FOLDOUT FRAME

RELATIVE INTENSITY OF N 45°E LINEATIONS
 DETERMINED BY PHOTOCELL SURVEY OF ERTS
 INTERPRETATION OF NW AND NE STRUCTURES

ERTS-1 ARIZONA MINERAL

For:
 NASA ERTS CONTRACT No. G-061

EARTH SATELLITE CORP.
 2150 SHATTUCK AVE., BERKELEY, CAL. 94704

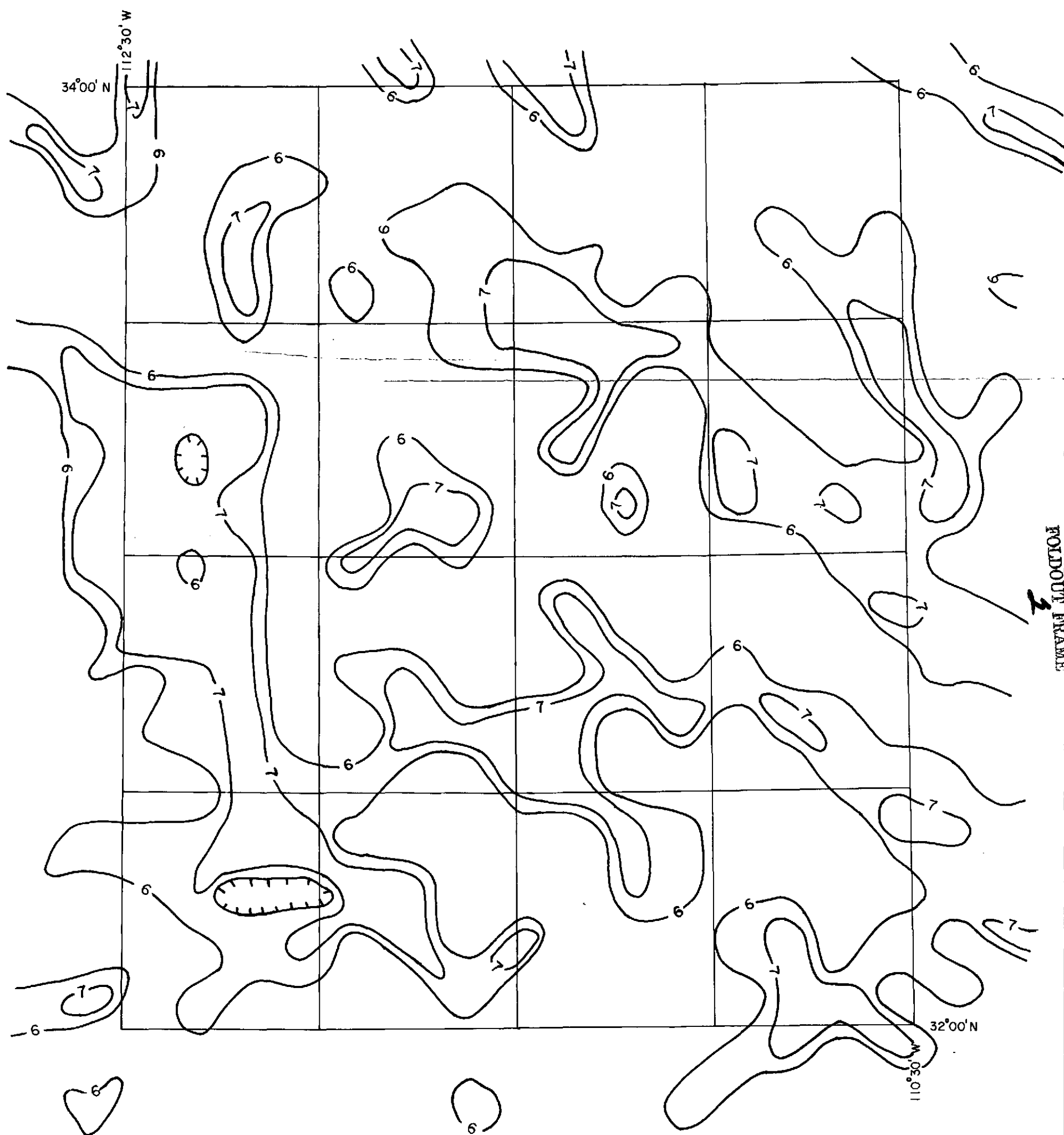
DATE: AUG 20, 1973	PLATE No 5	SCALE: 1:1,000,000	DRN. BY: JLW
-----------------------	---------------	-----------------------	-----------------

Earth Sat

50

FOLDOUT FRAME

N 50° W



FOLDOUT FRAME

FOLDOUT FRAME

Contour Intensity Equivalents
 6 (Meter Units) = 0.5 Foot Candles
 7 (Meter Units) = 1.0 Foot Candles
 CONTOUR INTERVAL ONE LUNA PRO LIGHT METER UNIT

RELATIVE INTENSITY OF N 50°W LINEATIONS
 DETERMINED BY PHOTOCCELL SURVEY OF ERTS
 INTERPRETATION OF NW AND NE STRUCTURES

ERTS-1 ARIZONA MINERAL

For:
 NASA ERTS CONTRACT No. G-061

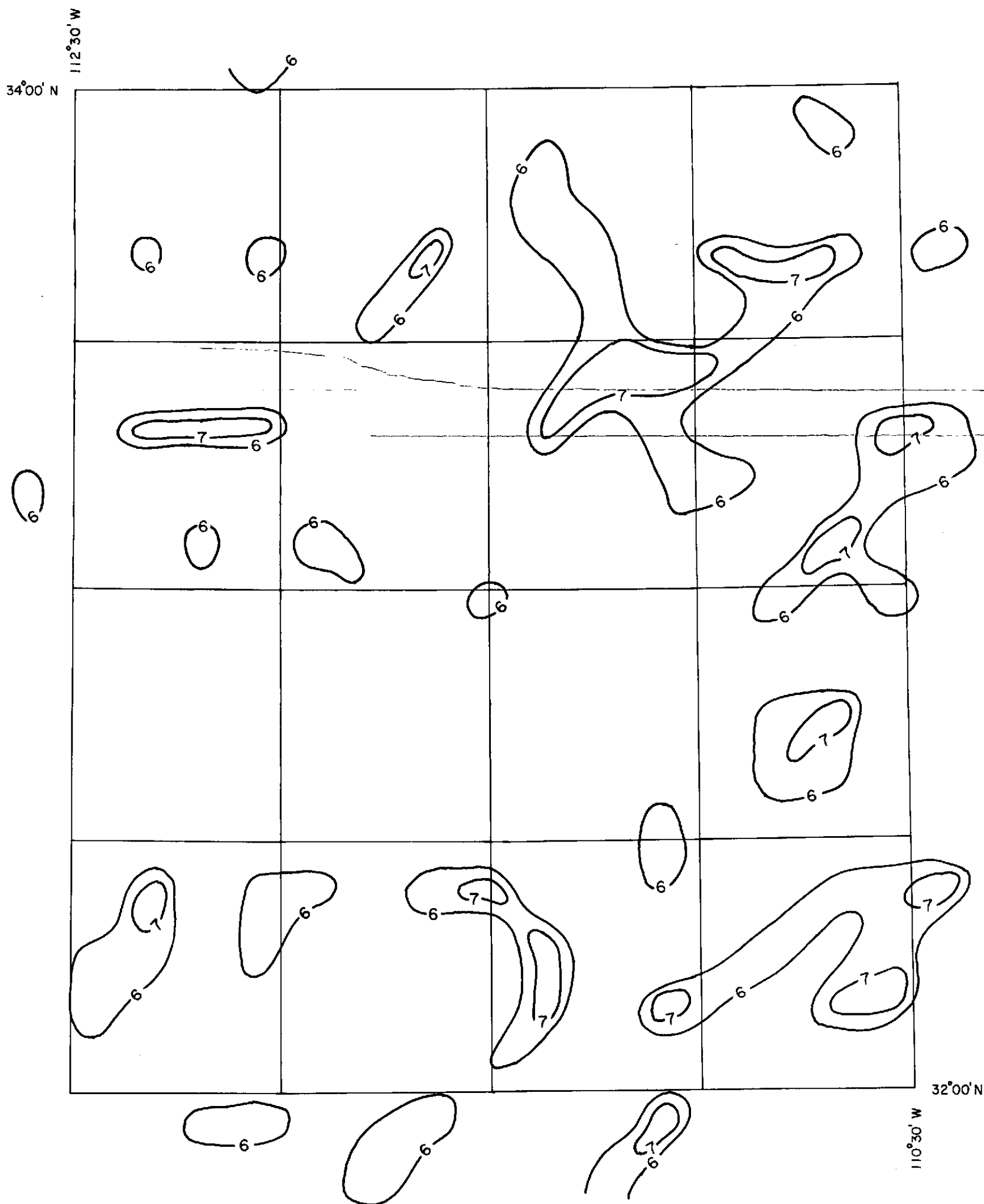
EARTH SATELLITE CORP.
 2150 SHATTUCK AVE., BERKELEY, CAL. 94704

DATE: AUG 20, 1973	PLATE No. 6	SCALE: 1:1,000,000	DRN. BY: JLW
-----------------------	----------------	-----------------------	-----------------

EarthSat

FOLDOUT FRAME

N 70°E



FOLDOUT FRAME

Contour Intensity Equivalents
6 (Meter Units) = 0.5 Foot Candle
7 (Meter Units) = 1.0 Foot Candle
CONTOUR INTERVAL - ONE LUNA PRO LIGHT METER UNIT

FOLDOUT FRAME

RELATIVE INTENSITY OF N 70°E LINEATIONS
DETERMINED BY PHOTOCCELL SURVEY OF ERTS
INTERPRETATION OF NS AND EW STRUCTURES

ERTS-1 ARIZONA MINERAL

For:
NASA ERTS CONTRACT No. G-061

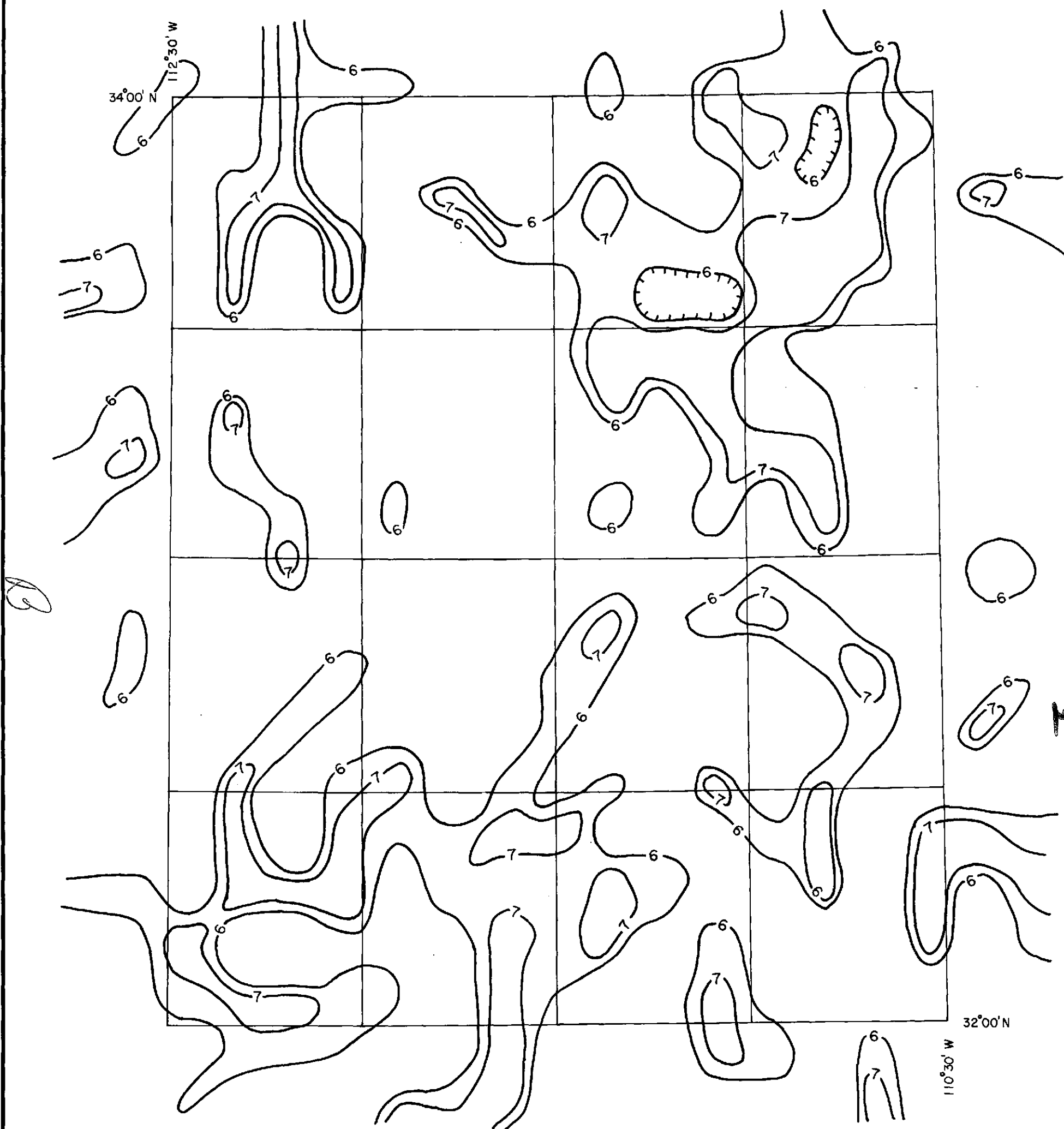
EARTH SATELLITE CORP.
2150 SHATTUCK AVE., BERKELEY, CAL. 94704

DATE: AUG 20, 1973	PLATE No. 7	SCALE: 1:1,000,000	DRN. BY: JLW
-----------------------	----------------	-----------------------	-----------------

EarthSat

FOLDOUT FRAME

N - S



FOLDOUT FRAME

Contour Intensity Equivalents
 6 (Meter Units) = 0.5 Foot Candle
 7 (Meter Units) = 1.0 Foot Candle
 CONTOUR INTERVAL - ONE LUNA PRO LIGHT METER UNIT

RELATIVE INTENSITY OF N-S LINEATIONS
 DETERMINED BY PHOTOCCELL SURVEY OF ERTS
 INTERPRETATION OF NS AND EW STRUCTURES

ERTS-1 ARIZONA MINERAL

For:
 NASA ERTS CONTRACT No. G-061

EARTH SATELLITE CORP.
 2150 SHATTUCK AVE., BERKELEY, CAL. 94704

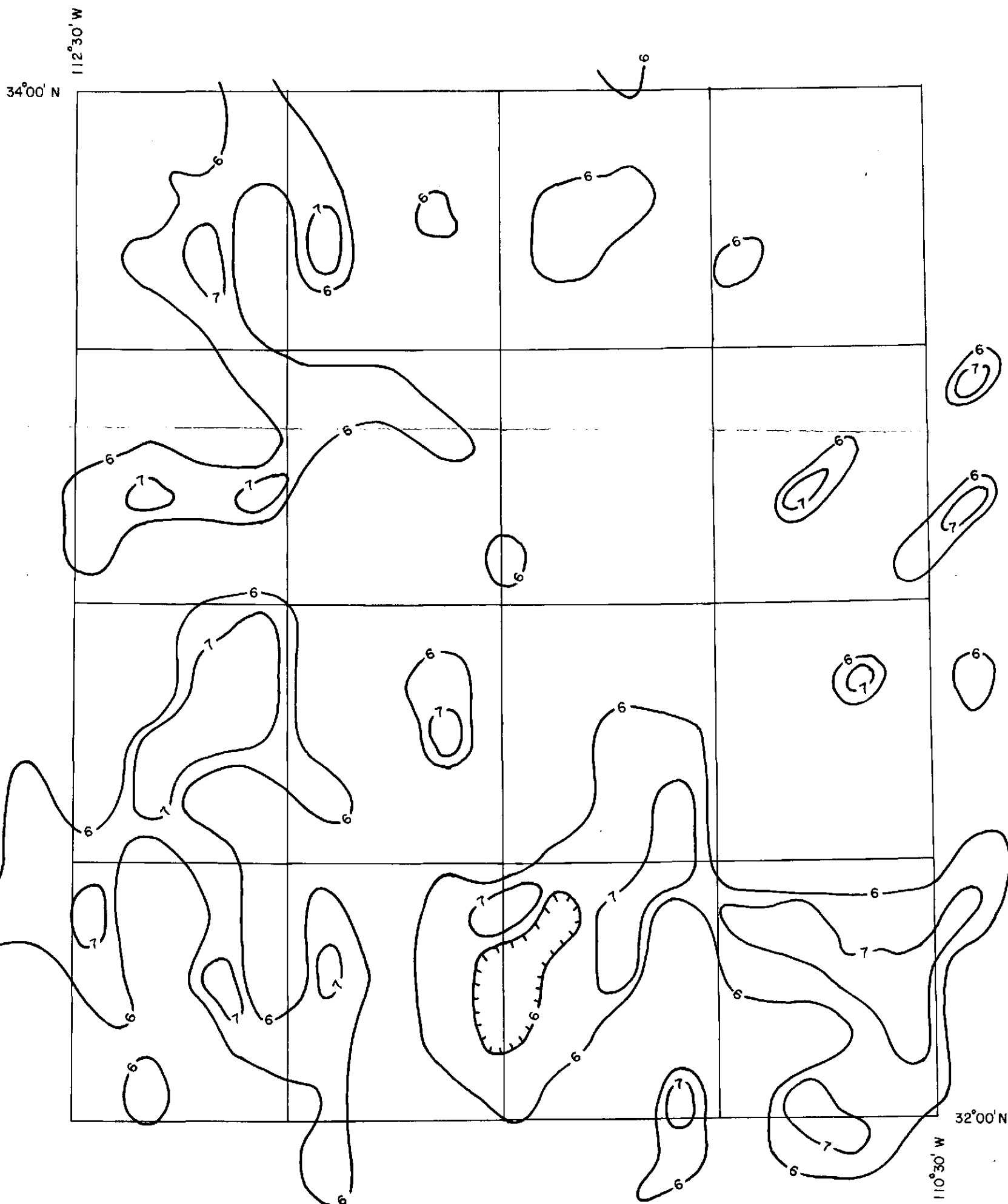
DATE: AUG 20, 1973	PLATE No: 8	SCALE: 1:1,000,000	DRN. BY: JLW
-----------------------	----------------	-----------------------	-----------------

EarthSat

FOLDOUT FRAME

62
 100

N 25° W



Contour Intensity Equivalents
6 (Meter Units) = 0.5 Foot Candle
7 (Meter Units) = 1.0 Foot Candle
CONTOUR INTERVAL - ONE LUNA PRO LIGHT METER UNIT

RELATIVE INTENSITY OF N 25° W LINEATIONS
DETERMINED BY PHOTOCCELL SURVEY OF ERTS
INTERPRETATION OF NW AND NE STRUCTURES

ERTS-1 ARIZONA MINERAL

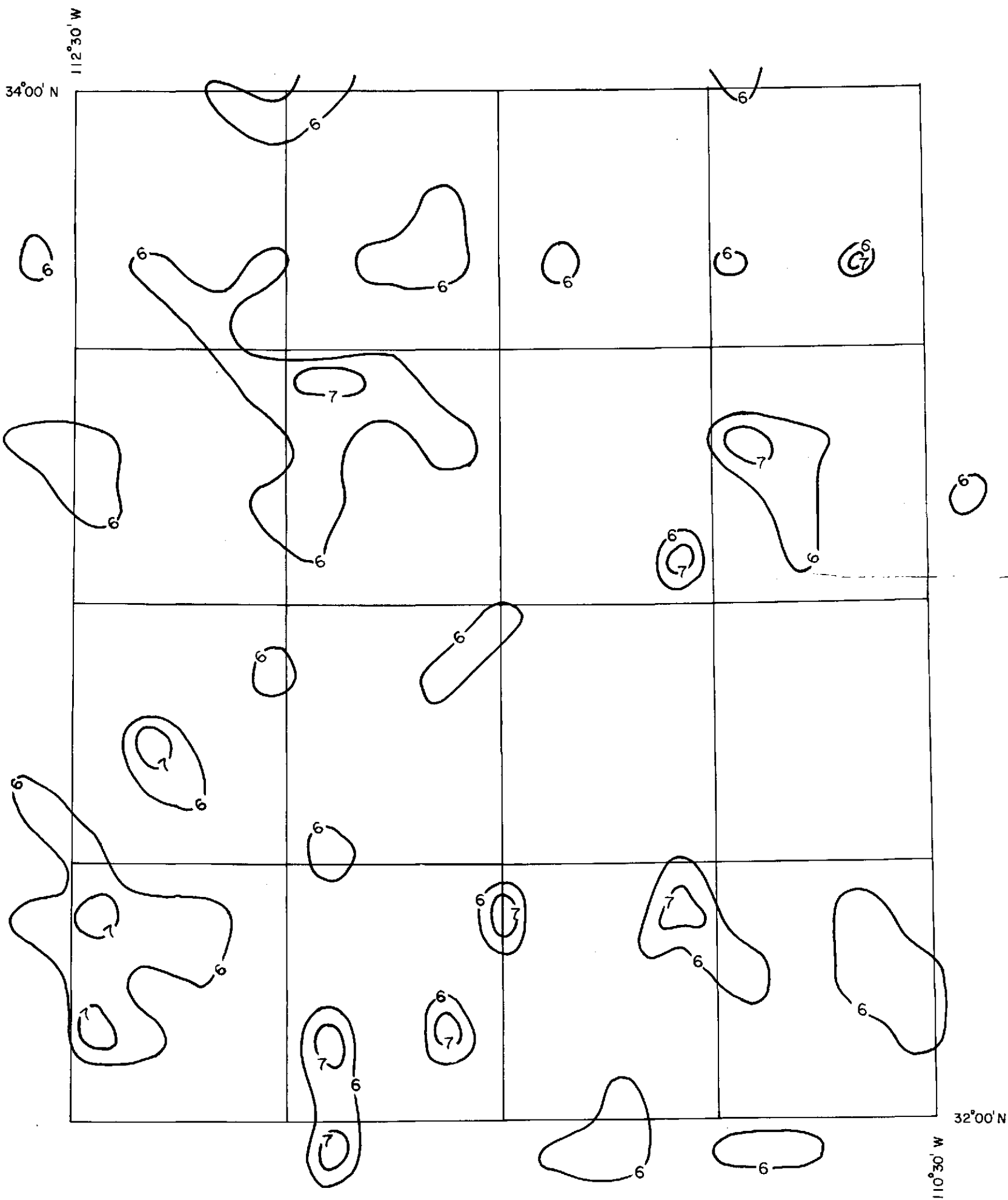
For:
NASA ERTS CONTRACT No. G-061

EARTH SATELLITE CORP.
2150 SHATTUCK AVE., BERKELEY, CAL. 94704

DATE: AUG 20, 1973
PLATE No. 9
SCALE: 1:1,000,000
DRN. BY: J L W

EarthSat

N 75° W



Contour Intensity Equivalents
6 (Meter Units) = 0.5 Foot Candle
7 (Meter Units) = 1.0 Foot Candle
CONTOUR INTERVAL ONE LUNA PRO LIGHT METER UNIT

RELATIVE INTENSITY OF N 75° W LINEATIONS
DETERMINED BY PHOTOCCELL SURVEY OF ERTS
INTERPRETATION OF NS AND EW STRUCTURES

ERTS-1 ARIZONA MINERAL

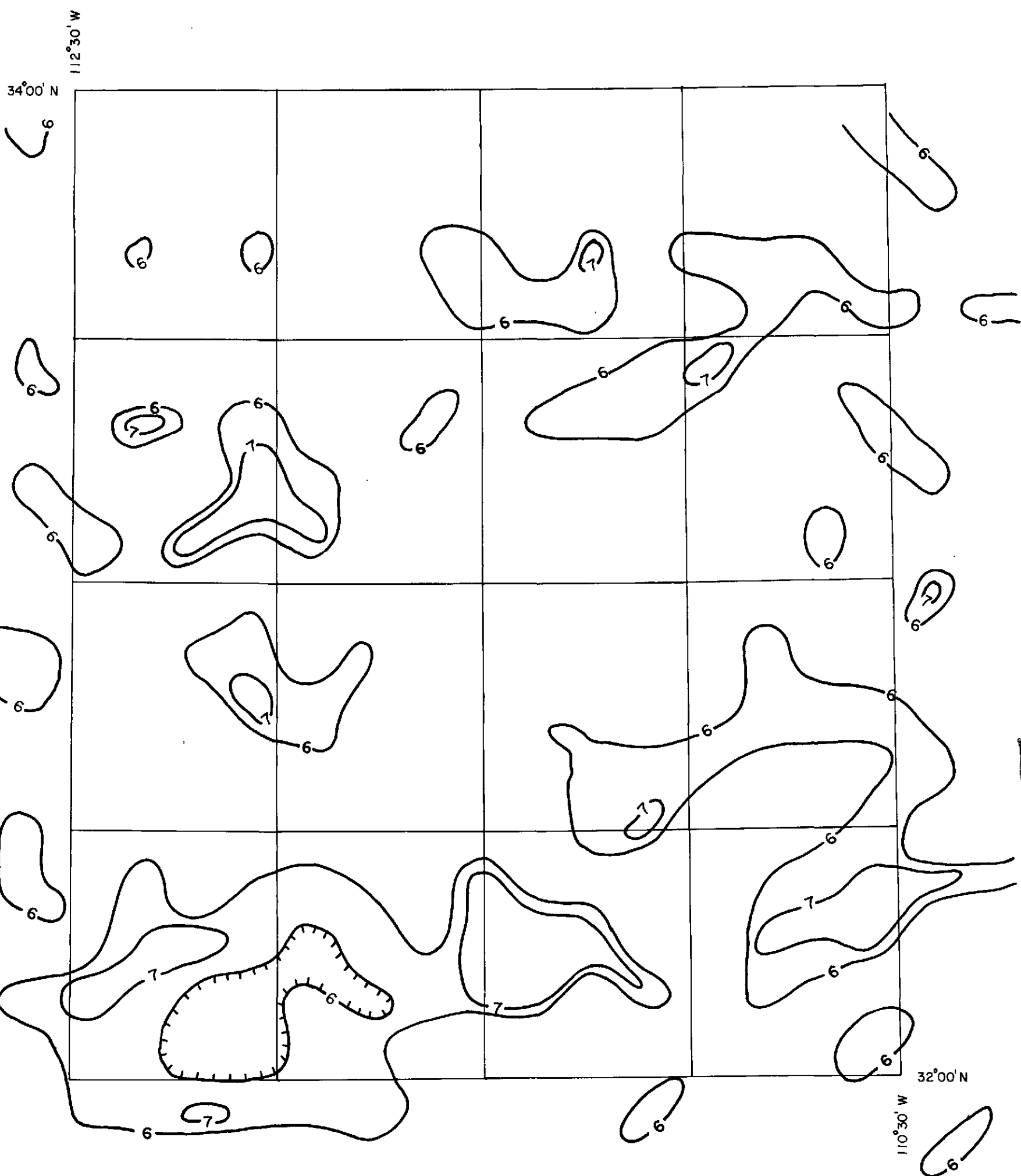
For:
NASA ERTS CONTRACT No. G-061

EARTH SATELLITE CORP.
2150 SHATTUCK AVE., BERKELEY, CAL. 94704

DATE: AUG 20, 1973	PLATE No. 10	SCALE: 1:1,000,000	DRN. BY: J L W
-----------------------	------------------------	-----------------------	-------------------

EarthSat

E - W



Contour Intensity Equivalents
 6 (Meter Units) = 0.5 Foot Candle
 7 (Meter Units) = 1.0 Foot Candle
 CONTOUR INTERVAL ONE LUNA PRO LIGHT METER UNIT

RELATIVE INTENSITY OF E-W LINEATIONS
 DETERMINED BY PHOTOCCELL SURVEY OF ERTS
 INTERPRETATION OF NS AND EW STRUCTURES

ERTS-1 ARIZONA MINERAL

For:
 NASA ERTS CONTRACT No. G-061

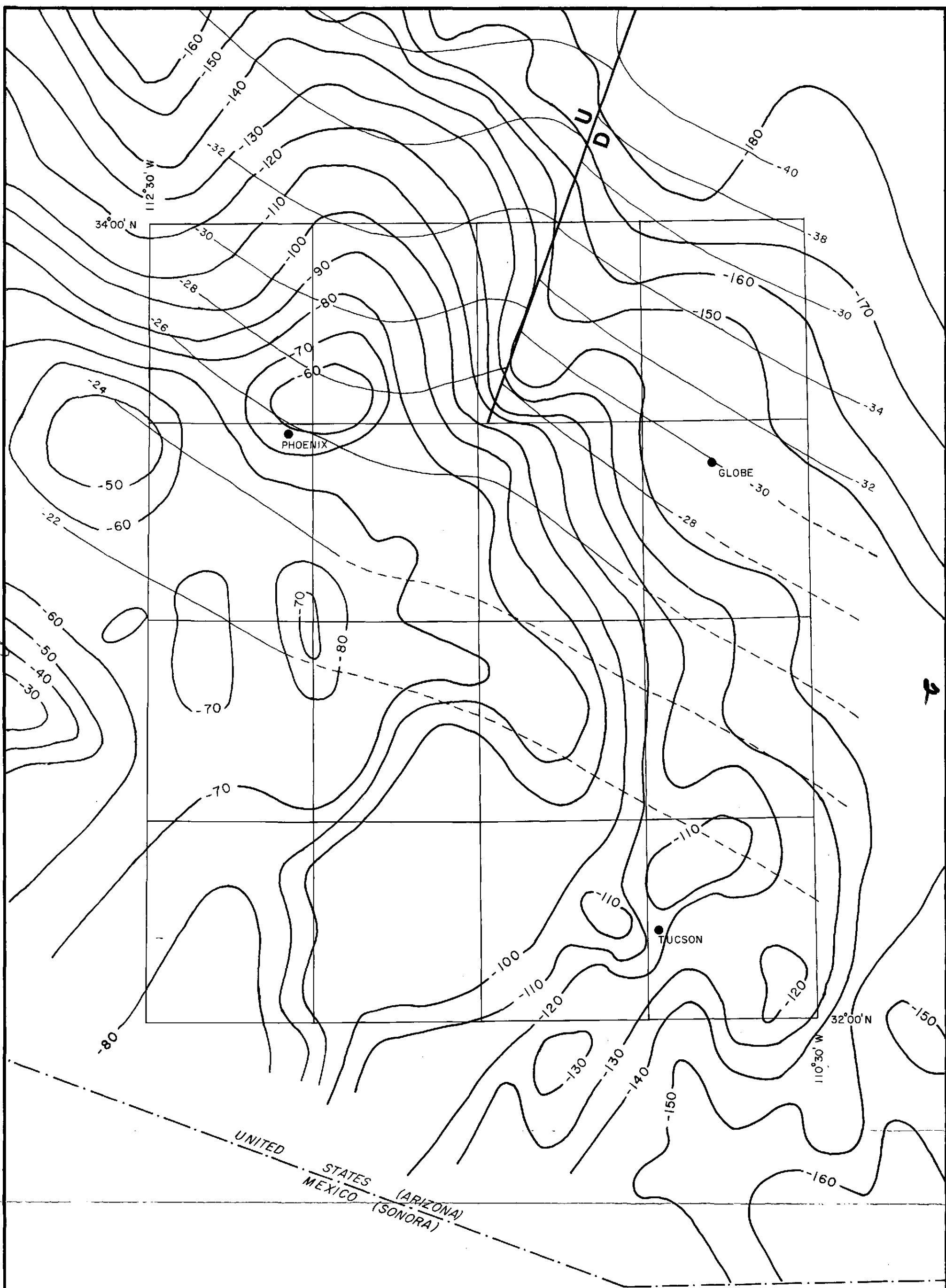
EARTH SATELLITE CORP.
 2150 SHATTUCK AVE., BERKELEY, CAL. 94704

DATE: AUG 20, 1973	PLATE No. 11	SCALE: 1:1,000,000	DRN. BY: JLW
-----------------------	-----------------	-----------------------	-----------------

EarthSat

2

9/6



LEGEND

Gravity - CI 10 mgals.

M-discontinuity - CI 2 km.; datum sea level

U ~ UP
 = FAULT
 D ~ DOWN

BOUGUER GRAVITY from - U.S. Geological Survey, 1959
 M-DISCONTINUITY modified from - Warren, 1969

BOUGUER GRAVITY and
 CONFIGURATION M-DISCONTINUITY

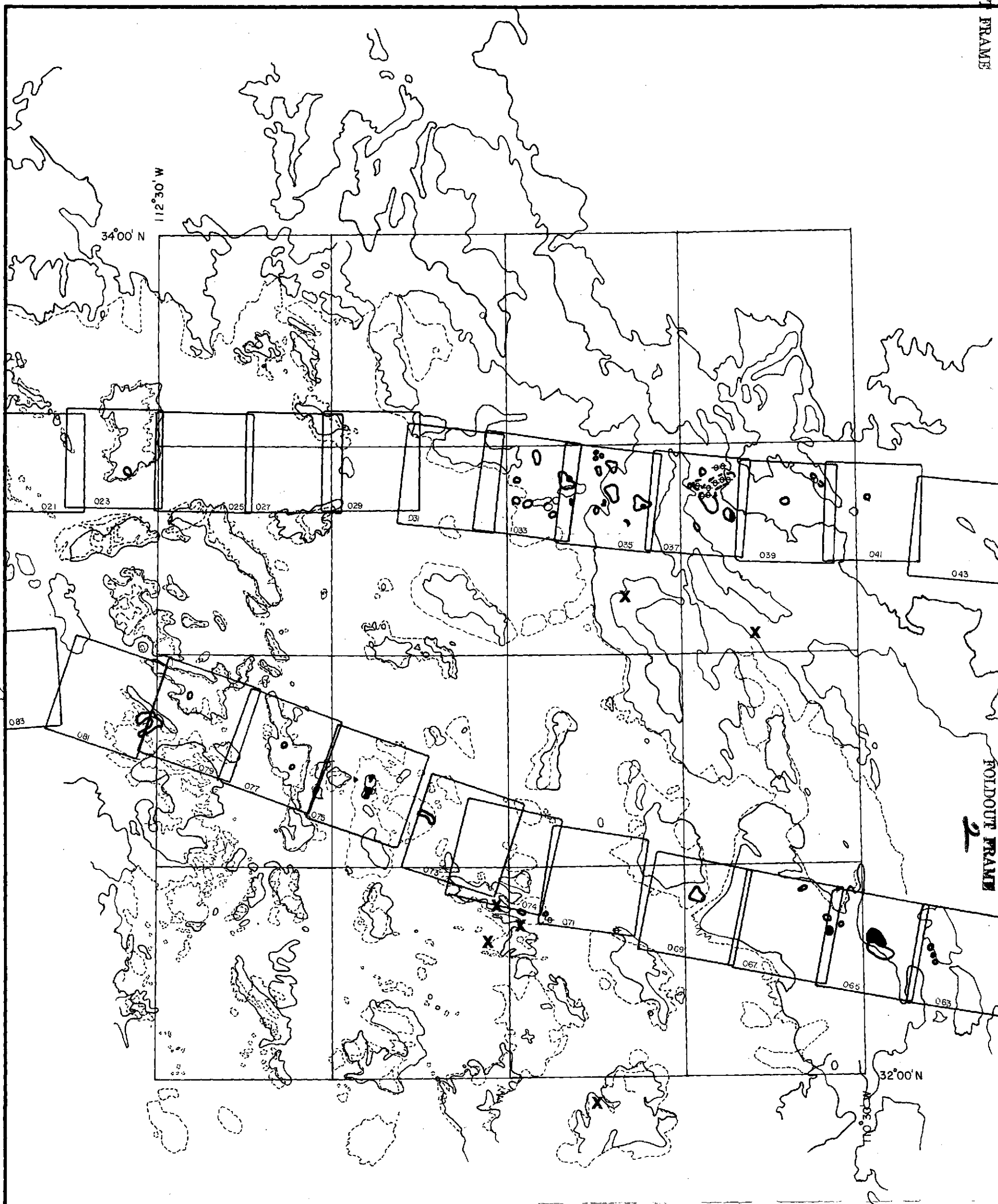
ERTS-1 ARIZONA MINERAL

For:
 NASA ERTS CONTRACT No. G-061

EARTH SATELLITE CORP.
 2150 SHATTUCK AVE., BERKELEY, CAL. 94704

DATE: AUG 20, 1973	PLATE No. 12	SCALE: 1:1,000,000	DRN. BY: J L W
-----------------------	-----------------	-----------------------	-------------------

EarthSat



EXPLANATION

HT (hydrothermal) ALTERATIONS from U-2 photography

○ BARELY POSSIBLE

● POSSIBLE HT

⊕ PROBABLE HT/MINE IDENTIFIED ON PHOTO.

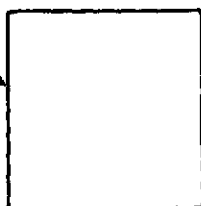
○ OUTCROP OF PRE-TERTIARY ROCKS AS SHOWN ON GEOLOGIC MAPS.

○ OUTCROP AREA SEEN ON ERTS MOSAIC.

HT (hydrothermal) alterations from ERTS Color Composites

✕ location mark

U-2 Photo locations from Mission 72-102



ALTERATION STUDY

ERTS-1 ARIZONA MINERAL

For:
NASA ERTS CONTRACT No. G-061

EARTH SATELLITE CORP.

2150 SHATTUCK AVE., BERKELEY, CAL. 94704

DATE:
AUG20,1973

PLATE No.
13

SCALE:
1:1,000,000

DRN. BY:
JLW

Earth Sat

FOLDOUT FRAME

FOLDOUT FRAME
2

FOLDOUT FRAME
3

34°00' N
112°30' W

32°00' N
110°00' W

EXPLANATION

- Faults (major)
- Faults (minor)
- XXXXXXX Magnetic Trends

DATA SOURCE: Residual Aeromagnetic Map of Arizona (1970 Ed.)

STRUCTURAL INTERPRETATION
FROM AEROMAGNETIC DATA

ERTS-1 ARIZONA MINERAL

For:
NASA ERTS CONTRACT No. G-061

EARTH SATELLITE CORP.
2150 SHATTUCK AVE., BERKELEY, CAL. 94704

DATE: AUG 20, 1973	PLATE No. 14	SCALE: 1:1,000,000	DRN. BY: J L W
-----------------------	-----------------	-----------------------	-------------------

EarthSat

59